JOURNAL OF ENVIRONMENTAL SCIENCES 127 (2023) 42–59

Available online at www.sciencedirect.com

ScienceDirect

www.elsevier.com/locate/jes

JES JOURNAL OF ENVIRONMENTAL SCIENCES

www.jesc.ac.cn

Review

Chemical reductive technologies for the debromination of polybrominated diphenyl ethers: A review

Ming Lei[1], *Yao Tang*[1], *Lihua Zhu*[2,*], *Heqing Tang*[1,*]

[1] *College of Resources and Environmental Science, South-Central Minzu University, Wuhan 430074, China*
[2] *School of Chemistry and Chemical Engineering, Huazhong University of Science and Technology, Wuhan 430074, China*

ARTICLE INFO

Article history:
Received 25 March 2022
Revised 6 May 2022
Accepted 10 May 2022
Available online 21 May 2022

Keywords:
Polybrominated diphenyl ethers (PBDEs)
Debromination
Chemical reduction
Electron transfer
Hydrogenation

ABSTRACT

Polybrominated diphenyl ethers (PBDEs) are widely used as brominated flame retardants, which had attracted amounts of attention due to their harmful characteristics of high toxicity, environmental persistence and potential bioaccumulation. Many chemical reductive debromination technologies have been developed for the debromination of PBDEs, including photolysis, photocatalysis, electrocatalysis, zero-valent metal reduction, chemically catalytic reduction and mechanochemical method. This review aims to provide information about the degradation thermodynamics and kinetics of PBDEs and summarize the degradation mechanisms in various systems. According to the comparative analysis, the rapid debromination to generate bromine-free products in an electron-transfer process, of which photocatalysis is a representative one, is found to be relatively difficult, because the degradation rate of PBDEs depended on the Br-rich phenyl ring with the lowest unoccupied molecular orbital (LUMO) localization. On the contrary, the complete debromination occurs easily in other systems with active hydrogen atoms as the main reactive species, such as chemically catalytic reduction systems. The review provides the knowledge on the chemical reductive technique of PBDEs, which would greatly help not only clarify the degradation mechanism but also design the more efficient system for the rapid and deep debromination of PBDEs in the future.

Introduction

Polybrominated diphenyl ethers (PBDEs) have been widely used as flame retardants in various field to inhibit or suppress combustion in matrices (Besis et al., 2012; De Wit et al., 2002). There are three kinds of commercial PBDE mixtures with varying numbers of bromine atoms, including Penta-BDE (primarily 2,2',4,4',5-pentabromodiphenyl ether (BDE99) (45%-50%) and 2,2',4,4'-tetrabromodiphenyl ether (BDE47) (38%-42%)), Octa-BDE (primarily 2,2',3,4,4',5',6-heptabromodiphenyl ether (BDE183)) and Deca-BDE (primarily 2,2',3,3',4,4',5,5',6,6'-

* Corresponding authors.
E-mails: lhzhu63@hust.edu.cn (L. Zhu), tangheqing@mail.scuec.edu.cn (H. Tang).

https://doi.org/10.1016/j.jes.2022.05.019
1001-0742/

decabromodiphenyl ether (BDE209)) (Wemken et al., 2019). Generally, the PBDEs were mainly added in polyurethane foam in furniture (65% of Penta-BDE), casings of electrical and electronic equipment (EEE) (80% of Octa-BDE), EEE and automotive seating (35% of Deca-BDE for each category) (Wemken et al., 2019). These compounds have been used since the 1970s, and China started the production of PBDEs in 1980s. Total consumption of Commercial Penta-, Octa-, and Deca-BDE in U.S. and Canada from 1970 to 2020 in products was evaluated to be ∼ 46,000, ∼ 25,000 and ∼ 380,000 tones, respectively (Abbasi et al., 2015). Total emissions of all PBDEs from the in-use product stock to air was estimated at 70–700 tones between 1970 and 2020, with annual emissions of 0.4-4 tones/year for each of Penta- and Octa-BDE and 3.5-3.5 tones/year for DecaBDE in 2014 (Abbasi et al., 2015).

There are complicated pathways of human exposure to PBDEs, mainly via dietary intake, ingestion of indoor air and dermal absorption (Tao et al., 2019). Meats and aquatic foods have been found to have the highest average sum PBDEs with values of 192.5 and 190.6 pg/g fresh weight, respectively (Xiong et al., 2019). Increasing evidence has indicated that PBDEs can disturb the balance of steroids *in vivo* and *in vitro* (Zhang et al., 2013), which may exert reproductive endocrine toxicity (Yu et al., 2015). Animal studies have further shown the neurodevelopmental and behavioral outcomes of exposure to PBDEs such as hepatic abnormality, endocrine disruption and possibly cancer (Liu et al., 2015; Shan et al., 2019; Yu et al., 2011). Their harmful characteristics of toxicity, combined with their environmental persistence and bioaccumulation potential brought them under the radar of environmental authorities (e.g., the European REACH (Registration, Evaluation, Authorisation and Restriction of Chemicals) regulation and Stockholm Convention) in the early 2000s, which resulted in the termination in the production of the commercial Penta- and Octa-BDE mixtures in 2004 and the commercial Deca-BDE by 2014 in North America. Correspondingly, Penta- and Octa-BDE were listed in Annex A of the Stockholm Convention in 2009, and Deca-BDE was listed in 2017 (Abbasi et al., 2019; Zhou et al., 2019). Despite the phase-out of PBDEs, their emission from in-use and waste stocks will continue until 2050 (Abbasi et al., 2019). Due to their high production volume, widespread usage, and environmental persistence, PBDEs have become ubiquitous contaminants in environmental media, biota and humans. As their levels are rapidly increasing in the environment, PBDEs have evolved from "emerging contaminants" to globally-distributed organic pollutants, it is urgent to develop the highly efficient methods for the pollution control of PBDEs.

In general, chemically strategies are more applicable than physical and microbial methods in terms of contaminants availability and toxicity, operation flexibility and remediation period (Ahmed et al., 2021; Nguyen et al., 2020). In terms of physical methods, landfill is commonly chosen as a means to treat PBDEs (Tongue et al., 2019). As an additive flame retardant, PBDEs were always mixed into products, and most of these products would become municipal solid waste (MSW) and be sent to landfills for dismantling or burying after being abandoned (Gallen et al., 2016). Due to no chemically bound in products, PBDEs are easily separated and released from MSW into soils and sediments, which result in producing potentially highly contaminated leachate (Zhang et al., 2021). For example, PBDEs have been detected in landfill leachate in many nations (4.0–351.2 ng/L in China, and 1010–21300 ng/L in Canada) (Currier et al., 2020; Harrad et al., 2019; Yao et al., 2021). Therefore, the physical technologies for the treatment did not fundamentally eliminate the potential emission of PBDEs. Biodegradation is considered as an economical and safe way for PBDEs removal (Huang et al., 2019; Ti et al., 2020). At present time, there are specific aerobic microorganisms that can be used to degrade PBDEs, but most of them could only act on the lower-brominated diphenyl ethers (Pan et al., 2019). Moreover, due to extreme hydrophobicity and sorptive binding with organic compounds in the soils, PBDEs are much regularly monitored under anaerobic conditions, where anaerobic microbes play the dominant role (Zhao et al., 2018). However, the reaction time required for anaerobic microorganisms was relatively long by comparing with the aerobic biodegradation, and only a few anaerobic microorganisms that could be used to degrade lower-brominated diphenyl ethers have been found (Pan et al., 2019). On the whole, owing to high hydrophobicity and low bioavailability of the compounds, the biodegradation efficiency of PBDE is relatively low, which could not avoid the potential harm of PBDEs for the environment.

In addition, higher-brominated PBDEs are relatively easy to be reduced by reductive species but resistant to be chemical oxidation. For example, Shi et al. conducted the oxidative degradation of BDE209 by potassium permanganate in concentrated sulfuric acid (Shi et al., 2015). Huang et al. used the photogenerated holes and hydroxyl radical to degrade BDE209 (Huang et al., 2013). The reaction conditions in oxidative systems are relatively harsh for the treatment of PBDEs. According to the abovementioned reasons, the investigation for the degradation of PBDEs mainly focused on the chemical reduction in this review. Especially, the reductive degradation thermodynamics, kinetics and mechanisms of PBDEs would be summarized in depth, which is essential for designing the efficient systems to remove PBDEs in real environment in the future.

1. Chemical reductive technologies for the treatment of PBDEs

Many chemical reductive techniques have been explored for the effective removal of PBDEs including photolysis, photocatalysis, electrocatalysis, zero-valent metal reduction and chemically catalytic reduction. By concentrating at the thermodynamics, kinetics and mechanisms of PBDEs degradation, we will illustrate a detailed and critical analysis is indicated for each degradation methodology as follows.

1.1. *Direct photolytic debromination of PBDEs*

The starting event for any photochemical reaction is the absorption of a photon by a molecule. Eriksson et al. reported the absorption spectra of seven typical PBDEs congeners with 4-10 bromine atoms (BDE209; 2,2',3,3',4,4',5,5',6-nonabromodiphenyl ether (BDE206); 2,2',3,4,4',5,5',6-octabromodiphenyl ether (BDE203); BDE183; 2,2',4,4',6,'-hexabromodiphenyl ether (BDE155);

2,2',3,4,4'-pentabromodiphenyl ether (BDE85); 3,3',4,4'-tetrabromodiphenyl ether (BDE77)), which suggested that the PBDEs could absorb the UV light with the maximum absorption wavelengths in the range of 290–310 nm (Eriksson et al., 2004). In the nature, sunlight would reach to the earth's surface after being absorbed and scattered by ozone, air and clouds. Subsequently, the PBDEs molecules existed in solvents or deposited in soil, sediment and dust would be excited by absorbing the photons with suitable energy, and the excited molecules may be then degraded through a serious of successive chemical reactions.

1.1.1. *Effect of key factors on the photolysis kinetics*

In photochemical reactions, the first step is the photoexcitation of chemicals, then an electron leaves from the highest occupied molecular orbital (HOMO) and arrives in the lowest unoccupied molecular orbital (LUMO). The second step of the reaction is between the photochemically excited state PBDEs molecules and another molecule in the ground state, which is generally referred as the hydrogen donor (solvents) (Wang et al., 2017a). That is to say, the photolysis of PBDEs is mainly affected by the properties of PBDEs themselves and the solvents when the light source is fixed.

Eriksson et al. studied the UV photolysis degradation of 15 individual PBDEs substituted with 4-10 bromine atoms, and found that the reactivity of PBDEs decreased with decreasing the number of bromine atoms in the PBDEs molecule, but with exceptions that was influenced by the PBDE substitution pattern (Eriksson et al., 2004). These exceptions suggested that the number of bromine atoms on the diphenyl ethers could not fully explain the photochemical reaction rules of PBDEs. In consideration of this, Wang and co-authors investigated the photodebromination behaviors of PBDEs in methanol/water systems, and found that the photodebromination kinetics of PBDEs congener with different brominated degree seem to only correlate with the LUMO energy (E_{LUMO}), but the PBDEs isomers are well correlated with the HOMO-LUMO gaps. Specifically, the PBDEs isomers with a narrower HOMO-LUMO gap and the PBDEs congener with a lower LUMO tend to degrade faster (Wang et al., 2017a).

Furthermore, the degradation rate was dependent on the used solvent (Table 1). According to the report of Eriksson et al. (2004), the photolysis rate of PBDEs in a methanol/water solution was around 1.7 times lower than in pure methanol, and 2-3 times lower than in tetrahydrofuran (THF). This difference was explained by the hydrogen donor effect of the solvent: as a "hydrogen donor", pure methanol is better than methanol/water, and THF is even better than methanol. Wang and co-authors also observed similar phenomenon, who found that the ratio of methanol/water in the mixture solvent is an important factor influencing the degradation rates of PBDEs. As the water content increased from 0 to 90%, the apparent rate constant value of PBDEs decreased from 0.0962 min^{-1} to 0.0134 min^{-1}. However, no relation could be obtained between the hydrogen donating or electron donating effects and the photolysis reactivity of PBDEs when more solvents were taken into consideration (Wang et al., 2017a). Xie et al. (2009) investigated the photolysis of BDE209 in various solvents such as THF, dichloromethane (DCM), isopropanol, acetone, ethanol, methanol, acetonitrile and dimethylsulfoxide (DMSO). The electronic structure of BDE209 in reaction field formed by solvents rather than hydrogen donating efficiency or electron donating efficiency of solvents were proved to be the decisive factors of the photolytic rate. The variations of both vertical excitation energy (E_{ex}) and the average formal charges of Br (q^{+}_{Br}) were resulting from the reaction fields formed by dipole/dipole interactions between the solvents and BDE209 molecules, which leads to a negative linear relationship between E_{ex} and log*k* and a positive linear relationship between q^{+}_{Br} and log*k* .

Other co-existed compounds may also affect the photolysis kinetics of PBDEs. For example, the addition of Triton X-100 (TX-100) as a surfactant increased the degradation rate of 4,4'-dibromodiphenyl ethers (BDE15) with a suitable concentration of, because TX-100 could act as hydrogen donor and photosensitizer (Huang et al., 2017). On the contrary, the presence of humic acid decreased the transformation of BDE209 adsorbed on the humic acid-coated sand by solar irradiation, because solar irradiation could only penetrate the first few millimeters of the sand and the humic acid may attenuate the light intensity (Hua et al., 2003).

In short, the factors affecting the photolytic degradation of PBDEs could be summarized as follows. (1) Light absorption of PBDEs molecules. The first step of the photolytic reaction is light absorption, and thus strengthening the light absorption of PBDEs molecules will accelerate the degradation rate of PBDEs. For example, the introduction of photosensitizer will increase the degradation rate of BDE15. (2) The structure of PBDEs molecules. The electrons will leave the HOMO orbitals to arrive at the LUMO orbitals after the PBDEs molecules absorb the suitable light. Therefore, the PBDEs congeners with a narrower HOMO-LUMO gap and a lower LUMO are much easier to form excited state molecules, followed by faster degradation. (3) The interactions between solvents and PBDEs molecules. The hydrogen donating or electron donating of solvents have no effect on the degradation of PBDEs, but the dipole/dipole interactions between the solvent and BDE209 molecules will affect the variations of both vertical excitation energy (E_{ex}) and the average formal charges of Br (q^{+}_{Br}), and there is a negative linear relationship between E_{ex} and log*k* and a positive linear relationship between q^{+}_{Br} and log*k*.

1.1.2. *Products and pathways in photolysis processes*

Photolytic degradation, at least initially, mainly seems to be a stepwise debromination process that the higher-brominated PBDEs were transformed to lower-brominated PBDEs and finally to diphenyl ether (DE) (Söderström et al., 2004). In the debromination process, the Mulliken atomic charges of bromine atoms of PBDEs has been proved to be a positive correlation with their degree of priority for releasing bromine atoms (Wang et al., 2017a). Taking the debromination of 2,2',4,4'-tetrabromodiphenyl ethers (BDE47) as an example, the bromine atom on the *ortho*-position with a higher Mulliken charge (-0.0735) is more susceptible compared to that on the *para*-position (-0.1140), thus the *ortho*-bromine on the phenyl ring that has more bromine substituents is preferentially removed (Wang et al., 2017a).

In addition to the transformation to lower-brominated diphenyl ethers then to diphenyl ether (DE), the other pathway is to generate polybrominated dibenzofurans (PBDFs) or DE

Table 1 – Comparisons between the photolytic debromination of PBDEs in various solvents.

Solvent	k (min^{-1})	PBDEs	Light source	Refs.
Methanol	0.0962±0.0011	BDE47	100 W mercury lamp	Wang et al. (2017a)
70% methanol-30% water	0.0559±0.0017	BDE47	100 W mercury lamp	Wang et al. (2017a)
50% methanol-50% water	0.0288±0.0014	BDE47	100 W mercury lamp	Wang et al. (2017a)
30% methanol-70% water	0.0178±0.0032	BDE47	100 W mercury lamp	Wang et al. (2017a)
10% methanol-90% water	0.0134±0.0022	BDE47	100 W mercury lamp	Wang et al. (2017a)
Methanol	7.2×10^5	BDE47	Fluorescent tube TL20W/09N	Eriksson et al. (2004)
Methanol-water	4.2×10^5	BDE47	Fluorescent tube TL20W/09N	Eriksson et al. (2004)
THF	1.2×10^6	BDE47	Fluorescent tube TL20W/09N	Eriksson et al. (2004)
Methanol	3.9×10^8	BDE209	Fluorescent tube TL20W/09N	Eriksson et al. (2004)
80% methanol-20%water	2.4×10^8	BDE209	Fluorescent tube TL20W/09N	Eriksson et al. (2004)
THF	4.98×10^8	BDE209	Fluorescent tube TL20W/09N	Eriksson et al. (2004)
Methanol	1.347×10^{-2}	BDE209	500 W Xe lamp	Xie et al. (2009)
Ethanol	1.974×10^{-2}	BDE209	500 W Xe lamp	Xie et al. (2009)
Isopropanol	1.656×10^{-2}	BDE209	500 W Xe lamp	Xie et al. (2009)
THF	2.737×10^{-2}	BDE209	500 W Xe lamp	Xie et al. (2009)
DCM	1.838×10^{-2}	BDE209	500 W Xe lamp	Xie et al. (2009)
DMSO	1.663×10^{-2}	BDE209	500 W Xe lamp	Xie et al. (2009)
Acetonitrile	1.528×10^{-2}	BDE209	500 W Xe lamp	Xie et al. (2009)
Acetone	1.18×10^{-3}	BDE209	500 W Xe lamp	Xie et al. (2009)

then to dibenzofuran (DF) (Wang et al., 2017a; Watanabe et al., 1987; Xie et al., 2009). It is noting that there was only lower-brominated PBDFs but with little accumulation of higher-brominated PBDFs. This indicates that reductive debromination rather than cyclization occurred in higher brominated diphenyl ethers by UV photolysis (Eriksson et al., 2004). Actually, it is not clear that the PBDFs is the main product or not, because only trace PBDFs could be detected in the photochemical systems. There are two possibilities for this phenomenon: (1) the cyclization reaction is really not the major route; (2) the PBDFs congeners have stronger absorbance at longer wavelengths than PBDEs, thus it has the higher decomposition rate and quantum yields than PBDEs and no accumulation in intermediates (Santos et al., 2016). Moreover, the mechanism for the formation of PBDFs also remains controversial. Eriksson et al. thought that the formation of the furan ring is possible for PBDEs of any level of bromination as long as one *ortho*-position is nonbrominated (Eriksson et al., 2004). On the contrary, Wang et al. indicated that the *ortho*-bromine substitution is the prerequisite for converting PBDEs into PBDFs. The PBDEs without an *ortho*-bromine substituent did not generate PBDFs, but sequentially debrominated to DE, which then converted into dibenzofuran (Wang et al., 2017a).

In addition, a little of oxidative intermediates could be also detected, which may be cautiously interpreted as deriving from hydroxylated or methoxylated products. For example, a methoxylated tetrabromodibenzofuran was observed in the photolysis of BDE209 in methanol/water (Eriksson et al., 2004). The *ortho*-hydroxydipenyl and *para*-hydroxydiphenyl were produced in the degradation process of BDE15 (Huang et al., 2017). Except for the abovementioned products, some undefined products would be generated by intermolecular polymerization in specific conditions (Hua et al., 2003; Xie et al., 2009).

The used solvents and matrix may influence the photolysis intermediates of PBDEs. Photolysis of BDE209 in methanol/water, pure methanol, ethanol, isopropanol and THF gave rise to an almost identical set of products, and most of products were identified as lower-brominated diphenyl ethers, while few lower-brominated diphenyl ethers were detected in acetonitrile and CCl_4 (Xie et al., 2009). In the photolysis process of BDE209, no tetra-BDFs or penta-BDFs were seen in the silica gel extracts, while in the soil and sand samples tetra-BDFs, penta-BDFs and hexa-BDFs were seen, but no hepta-BDFs were found (Söderström et al., 2004).

In summary, the direct photolysis of PBDEs is too time-consuming and energy-consuming to be applied in the real engineering, but it could be used for evaluating the potential risks of these contaminants in real environment.

1.2. *Photocatalytic reductive debromination of PBDEs*

Semiconductor photocatalytic reduction has been applied to solve a variety of problems of environmental interest in addition to water and air purification (Abdullah et al., 2017; Linsebigler et al., 1995; Li et al., 2019; Tugaoen et al., 2018). The mechanism of semiconductor photocatalysis may be described as follows by taking TiO_2 as the example: TiO_2 photocatalysts act as sensitizers for light-reduced redox processes due to their electronic structure, which is characterized by a filled valence band (VB) and an empty conduction band (CB). When a photon with an energy of $h\nu$ matches or exceeds the bandgap energy (Eg) of the semiconductor, it would be excited to produce an electron in CB (e^-_{CB}) and a hole in VB (h^+_{VB}) (Eq. (1)). These charge carriers can rapidly migrate to the surface where they are captured by suitable electron donors/acceptors (Eqs. (2) and (3)), and/or recombine, dissipating into heat and/or light (Eq. (4)) (Linsebigler et al., 1995; Lei et al., 2014).

$$TiO_2 + h\nu \rightarrow e^-_{CB} + h^+_{VB} \quad (1)$$

$$h^+_{VB} + \text{electron acceptors} \rightarrow \text{oxidative products} \quad (2)$$

$$e^-_{CB} + \text{electron donors} \rightarrow \text{reductive products} \quad (3)$$

$$e^-_{CB} + h^+_{VB} \rightarrow \text{light or heat} \quad (4)$$

1.2.1. *UV photocatalytic debromination*

One of the extensively investigated methods for the treatment of PBDEs is the photocatalytic reduction by UV light, which mainly focuses on the TiO_2-mediated photolysis. The reductive degradation of PBDEs is a consequence of their reaction with the conduction band electrons and/or the other reducing species.

Sun et al. (2009) reported the photocatalytic degradation of PBDEs for the first time. Rapid degradation of BDE209 occurred in the anoxic BDE209/TiO_2 dispersions under UV irradiation (λ > 365 nm), and more than 90% of BDE209 disappeared after 7.5 min of irradiation. However, the debromination efficiency of BDE209 was relatively low, and hence the hepta- and hexa-BDEs were the dominant intermediates after irradiation for 9 hr, and hexa-BDEs were observed as major products after 24 hr irradiation. In other words, the TiO_2-mediated photocatalytic system is beneficial to the debromination of higher-brominated PBDEs, but ineffective to lower-brominated PBDEs. In the photocatalytic reduction, debromination of PBDEs may be initiated through two possible pathways: (1) direct electron transfer from the conduction band of TiO_2; (2) addition of a hydrogen atom to an aromatic carbon. Following both initial steps is the elimination of bromine (Sun et al., 2009). With the aid of DFT calculations, the one-electron reduction of PBDEs rather than the hydrogenolysis pathway was indicated to be the initial step (Sun et al., 2009). For this reason, many strategies have been used to modify TiO_2 catalysts for the debromination of PBDEs, which could be roughly divided into three types: (1) accelerating the separation of electron-hole pairs and improving the number of effective electrons (Hu et al., 2017; Lei et al., 2014, 2016a, 2016b; Wang et al., 2019); (2) increasing the reductive potential of conduction band electrons (Lei et al., 2016b; Chen et al., 2020); and (3) strengthening the interaction between the catalyst and PBDEs, and weakening the bond energy of C-Br bond in PBDEs (Lei et al., 2016a; Li et al., 2014; Lv et al., 2016).

The photocatalytic debromination on TiO_2 is an interfacial electron transfer process, and hence the improving of debromination efficiency requires primarily an enhanced charge separation of TiO_2. To enhance the charge separation of TiO_2, surface modifications such as depositing metal or metal oxide (Hu et al., 2017; Lei et al., 2016a, 2016b; Wang et al., 2019b), combining carbon materials have been developed. By depositing TiO_2 nanoparticles on reduced graphene oxide (RGO), Lei et al. (2014) prepared RGO/TiO_2 to yield a debromination efficiency of 59.4% of BDE209 at 12 hr of UV irradiation, being 4 times that of naked TiO_2. The enhancement of debromination efficiency was attributed to that RGO not only trapped electrons to improve the charge separation on TiO_2, but also shuttled the accumulated electrons to initiate multi-electron transfer to BDE209 (Lei et al., 2014). Wang et al. synthesized the metal doped titanium dioxide (i.e., Ag/TiO_2, Cu/TiO_2) and investigated for their effectiveness to degrade PBDEs under UV light (Wang et al., 2019b). The deposition of metal greatly enhanced the performance of TiO_2 to degrade PBDEs, because it would prevent the recombination of electron and holes, and the electrons would be accumulated in the metal surface and then transferred to the pollutant, which is similar to the results of Lei et al. (2016a). Moreover, some metal oxides such as CuO and Cu_2O could be used to promote the separation of electron-hole pairs by the formation of heterojunction, consequently improving the debromination performance of TiO_2 (Lei et al., 2016b; Hu et al., 2017).

There is a good correlation between the reduction rates and the energy level for the lowest unoccupied molecular orbital (E_{LUMO}) of the PBDEs was usually observed in an earlier study (Hu et al., 2005). For example, BDE47 (E_{LUMO} = -1.518 eV) has a much lower electron affinity than BDE209 (E_{LUMO} = -2.419 eV). As a consequence, amounts of lower-brominated diphenyl ethers would be accumulated accompanied with the degradation of higher-brominated diphenyl ethers (Sun et al., 2009). Thereby, it is essential to increase the reductive potential of conduction band electrons to achieve the transformation of PBDEs to diphenyl ethers. Lei et al. (2016b) proposed a concept of "switching reduction potential by the valence state of copper". By the in-situ change from CuO to Cu_2O induced by irradiating CuO/TiO_2, the newly produced Cu_2O/TiO_2 composite possessed a more reductive energy for injecting electrons to lower-brominated diphenyl ethers due to that the conduction band of Cu_2O lies more negative than that of TiO_2 and CuO . Therefore, the degradation rate constant of the photocatalytic reduction of BDE209 and BDE47 were evaluated as 1.99 and 0 min^{-1} on TiO_2 respectively, but these values were significantly increased to 3.19 and 0.41 min^{-1} on CuO/TiO_2. It should be emphasized that there was a short induction period needed for the transformation of CuO/TiO_2 to Cu_2O/TiO_2 in the photocatalytic reduction of BDE47 (**Fig. 1**). Based on the similar principle, Chen et al. successfully synthesized the Z-scheme Cu_2O-(rGO-TiO_2) for the reductive removal of BDE47. The results of characterization confirmed that the electron transfer in Cu_2O-(rGO-TiO_2) followed a Z-scheme pathway, and the reduction processes that induced the reductive degradation of BDE47 occurred in the conduction band of Cu_2O (Chen et al., 2020).

The cleavage of C-Br bond on the surface of the photocatalysts is a key step in the debromination of PBDEs. Li et al. conducted UV photocatalytic degradation of BDE209 on titanium dioxide with surface-loaded palladium (Pd-TiO_2), and found that the loaded Pd could trap the photogenerated electrons of TiO_2 to enrich on its surface, and the further transfer of the electron to PBDEs by assisting the cleavage of the C-Br bond owing to the high affinity of Pd metal for bromine atoms. Li et al. (2014) further proposed an "Ag-promoted electron transfer and C-Br cleavage" concept in the photocatalytic degradation of BDE47 with Ag/TiO_2 as the photocatalysts. There is almost no BDE47 removal observed on TiO_2 after a 25 min UV irradiation, but the photocatalytic reduction of BDE47 was much enhanced after 13 min with a short induction period (9 min) and a fast degradation period (4min). In this system, Ag nanoparticles needed an induction period to transfer and accumulate the electrons of TiO_2 conduction band, which resulted in a shift in the Fermi level to a more reductive energy level and the stretch of C-Br bond due to the affinity of Ag to Br atoms (**Fig. 2**) (Lei et al., 2016a). In addition, the presence of metal copper nanoparticles as co-

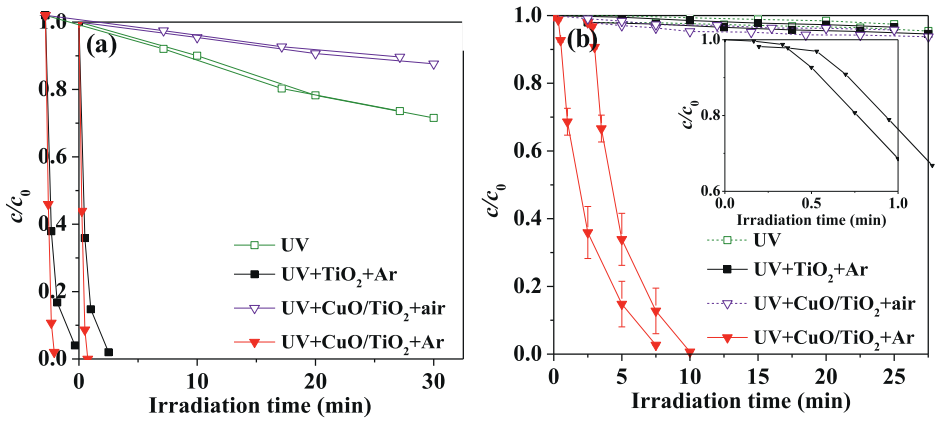

Fig. 1 – Photocatalytic degradation of (a) BDE209 in methanol and (b) BDE47 in a methanol-water (7:3) mixture. BDE209 undergoes efficient degradation, but the photocatalytic reaction for BDE47 was not observed in UV-irradiation anoxic TiO_2 suspensions. Whereas, the degradation efficiency of almost 100% within 0.75 min and 7.5 min for BDE209 and BDE47 on CuO/TiO_2 in the UV-irradiation anoxic atmosphere. In addition, the rapid degradation of BDE209 occurred on CuO/TiO_2 at the early reaction stage, but there was a short induction period (20 sec) needed in the photocatalytic degradation of BDE47 (the inset in b) (Lei et al., 2016b).

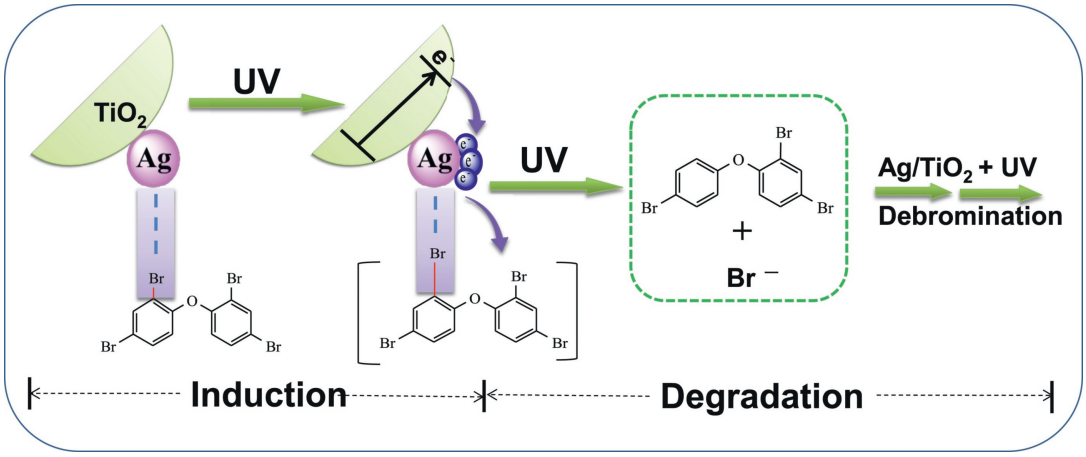

Fig. 2 – A mechanism for the initiation and development of photocatalytic degradation of BDE47 on Ag/TiO_2.The affinity between Br atoms and Ag enhances the adsorption of BDE47 on the Ag particles in Ag/TiO_2. Prior to BDE47 reduction, Ag^0 nanoparticles need an induction period to enrich amounts of electrons to shift the Fermi level and elongate the C-Br bond until charged $Ag^0(ne^-)$ nanoparticles transferred the electron to BDE47 by assisting the cleavage of the C-Br bond. Beyond the induction time, the debromination of BDE47 goes very rapidly (Lei et al., 2016a).

catalysts could also greatly enhance the adsorption of PBDEs and be position-specifically activate the C-Br bonds during the electron-transfer process (Lv et al., 2016).

On the whole, the abovementioned methods for the modification of TiO_2 showed enhanced degradation of lower-brominated diphenyl ethers such as BDE47. The degradation efficiency of BDE47 could reach up to 100% within several minutes of irradiation (Lei et al., 2016a, 2016b). However, the complete debromination of PBDEs is rather difficult, because the reactivity of the debromination of PBDEs decreases with the decreasing Br number in PBDEs (Keum et al., 2005; Zhuang et al., 2010). For example, the BDE47 molecules only could be reduced to 2,4,4'-tribromodiphenyl ether (BDE28) or 4,4'-dibromodiphenyl ether (BDE15) over Ag/TiO_2, CuO/TiO_2 or RGO/TiO_2, but the further debromination of these intermediates was too slow to be observed (Lei et al., 2016a, 2016b, 2018b). Indeed, unlike the generally accepted summary that the degradation rate constant (k_R) of PBDEs is dependent on the total Br number of PBDEs, k_R is found to depend on the Br number on a phenyl ring with more Br atoms than the other one due to the LUMO localization on the Br-rich phenyl ring (**Fig. 3**) (Guo et al., 2019). For example, the k_R of BDE209 is 2×10^7 times larger than that of BDE15. As a result, the deep debromination of PBDEs to DE was confirmed to be difficult through an electron-transfer process. It was worth noting that the rapid and deep debromination of PBDEs was achieved over $Pd\text{-}TiO_2$ under the UV light (Li et al., 2014), we assumed that its mechanism for reductive debromination was much different

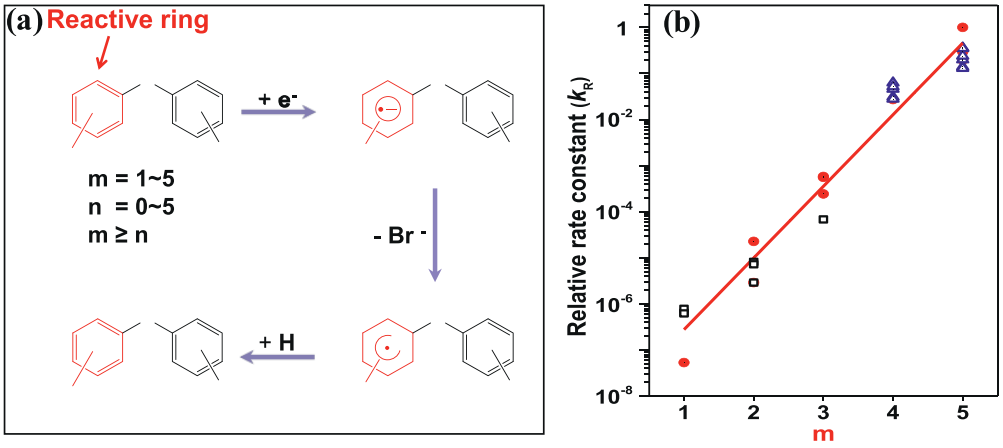

Fig. 3 – (a) A scheme for the preferable debromination of PBDEs on the ring with more Br atoms, where the two phenyl rings are assigned to "m ring" and "n ring", which represent the phenyl ring with more and less Br atoms, respectively. (b) A linear dependence of the relative degradation rate constant of PBDEs on the m value in an electron-transfer process. The relative rate constant of PBDEs are mainly dependent on the number of m in an electron-transfer process, where the data were, respectively obtained from UV photocatalytic degradation of PBDEs on CuO/TiO_2 (solid squares) (Guo et al., 2019), degradation by zero-valent iron (open triangles) (Keum et al., 2005) and degradation by sodium borohydride (open squares) (Granelli et al., 2012).

from the others photocatalytic system due to the specific role of Pd nanoparticles.

1.2.2. Visible-light photocatalytic debromination

Most studies about the photocatalytic debromination of PBDEs are focused on the TiO_2-based photocatalysis under UV irradiation. However, only 5% of the solar spectra belongs to UV light. In order to make the best use of solar light, it is necessary to explore the photocatalytic system for the debromination of PBDEs under visible light, which accounts for about 50% of the solar light. In recent years, some methods were developed for the debromination of PBDEs, and one of the most important methods is depended on the semiconductor with narrow band gaps such as g-C_3N_4 (Lei et al., 2020b; Shao et al., 2018; Wei et al., 2019), Cu_2O (Miller et al., 2017), CdS (Wang et al., 2019b) and so on. g-C_3N_4 possesses a band gap of 2.7 eV with excellent visible light activity, and its conduction and valence band energy are about -1.1 V and 1.6 V (versus normal hydrogen electrode) (Wang et al., 2009). Nevertheless, the bulk g-C_3N_4 always showed a low quantum efficiency in practical application due to the easy recombination of photogenerated carriers. For this reason, Shao et al. investigated the enhanced photoreduction degradation of PBDEs with Fe_3O_4-g-C_3N_4 under visible light irradiation due to the heterojunction between g-C_3N_4 and Fe_3O_4. More than 60% of BDE209 were removed after 1 h of irradiation, and the degradation rate constant over Fe_3O_4-g-C_3N_4 has been 6.7 times than the pure g-C_3N_4 (Shao et al., 2018). In the terms of the activation of C-Br bond, Wei et al. (2019) developed a catalytic system based on metallic Ni loaded on g-C_3N_4 that accomplished the complete debromination of BDE47 with triethylamine as the activity directing agent, and the debromination efficiency could reach up to 97.5% after 24 hr of irradiation because triethylamine could activate the C-Br bond via either nucleophilic attack by surface hydrogen/hydride species on the Ni surface or oxidative addition to the Ni site and promote the weakening of C-Br bond. In order to further increase the reactivity of PBDEs over the photocatalysts, Lei et al. (2020b) prepared Pd/g-C_3N_4 with a simple impregnation-chemical reduction method for the complete debromination of BDE47. Under optimal reaction conditions, all the added BDE47 (10 μmol/L) was transferred to free-bromine products in methanol-water mixture with an illumination of 60 min (**Fig. 4**) . Pd nanoparticles exerted affinity interaction with bromine atoms and storing of electrons on Pd would increase the binding interaction, which accelerated the cleavage of C-Br bond. It was worth noting that the active hydrogen atoms rather than electrons played an important role on the complete debromination of PBDEs in the Ni or Pd-mediated photocatalytic systems.

In addition, there are many other visible-light-driven photocatalysts used for the reduction of PBDEs. For example, Cu_2O and Pd as the main catalysts and co-catalysts was utilized for the photocatalytic reductive debromination of PBDEs, and Cu_2O@Pd yielded the effective debromination of BDE47 with rate constant of 0.21 hr^{-1} (Miller et al., 2017). Cu_2O may produce H_2 from H_2O under visible light irradiation, and the evolved H_2 is subsequently activated by Pd to achieve the reductive debromination of PBDEs. Wang et al. reported that the degradation and debromination of BDE47 was efficiently achieved using Ag/CdS under visible light with a degradation efficiency of 100% and a debromination ratio of 44.3% within 30 min (Wang et al., 2019c). Shao et al. used AgI/TiO_2 as photocatalysts to degrade BDE209 with the reaction rate constant of 0.29 ± 0.02 hr^{-1}. The special structure of AgI-TiO_2 performs remarkably enhanced electron transfer, multi-electron transfer, and results in high photocatalytic activity (Shao et al., 2017). RGO could be also exhibited high reactivity for the degradation of BDE209. The hydrophobic interaction, π-π interaction, and halogen-binding interaction between PBDEs and RGO enable the photogenerated electrons transfer from the RGO to PBDEs

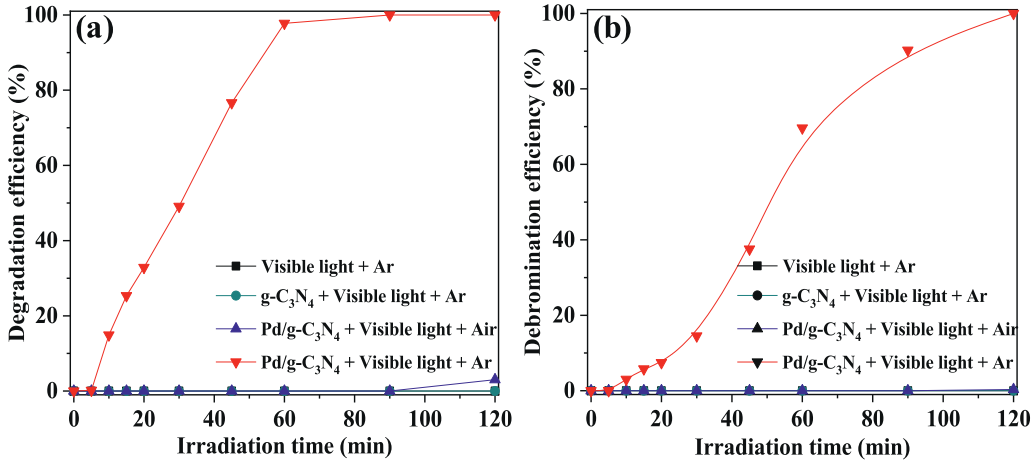

Fig. 4 – (a) Degradation and (b) debromination efficiency of BDE47 with an illumination of visible light in various system. The degradation efficiency of BDE47 was reached to 97.8% after 50 min, and all the bromine atoms were removed after 120 min of visible-light irradiation over Pd/g-C_3N_4 in Ar-saturated methanol-water (V:V = 7:3) solution (Lei et al., 2020b).

and lead to the efficient reductive debromination of BDE209 (Sheng et al., 2018).

In general, the photocatalytic mechanism of PBDEs under the visible light is similar to that under the UV light, both of which are mainly induced by photogenerated electrons except that the Pd nanoparticles was used as co-catalysts. Some strategies, such as fabricating the heterojunction by loaded the metal or metal oxides, enhancing the interaction between catalysts and PBDEs molecules and so on, may be used to increase the number of electrons and weaken the bond energy of C-Br bond. Compared with the photocatalytic process under UV light, the photocatalytic degradation of PBDEs is induced by visible light with using the semiconductors with narrow band gaps as catalysts, which favors the treatment of PBDEs in real environment. However, the high recombination rate of electron-hole pairs and the photo-instability of the semiconductor with narrow-band may be the main problem to be aimed at in the future.

1.2.3. *Products and pathways in photocatalytic systems*

Generally, the PBDEs was transformed to its lower-brominated congeners in a stepwise way in the photocatalytic systems. The catalysts and external electron/hydrogen donors forms active species that initiate C-Br bond activation via electron-transfer, nucleophilic attack by hydrogen/hydride species or oxidative addition with an illumination of light (Wei et al., 2019).

The intermediates identification in the TiO_2-mediated system shows that the bromine atoms at *ortho* or *meta* positions are more susceptible to be released than those at the *para* position, which may be ascribed to that the most likely initial step for the reduction of BDE209 is the one-electron transfer process and the calculated bond dissociation energy of C-Br bond at *ortho* position is the lowest (Sun et al., 2009). The position-selectivity of debromination has been well confirmed with Ag/TiO_2 and CuO/TiO_2 as photocatalysts (Lei et al., 2016a, 2016b). The debromination of BDE47 may be initiated by gaining an electron and the additional electron likely enters the most positively charge *ortho*-carbon to form the radical $BDE47^{-\bullet}$, then the C-Br bonds at the *ortho*-positions is significantly lengthened and even broken to release bromine atoms (Lei et al., 2016a). Unfortunately, the further debromination intermediate is difficult to be detected due to their weak electron affinity of lower-brominated congeners as described above, but most of the photocatalytic systems until the present time tend to follow the electron-transfer process. Except for the stepwise debromination, it is worth noting that the debromination by electrons may skip some reduction steps. For example, Lei et al. (2014) illustrated the changes in homologue distribution with reaction time in the UV-RGO/TiO_2 system, and found that the relative distribution of PBDEs products varies with extending UV time, e.g., 7Br, 9Br and 6Br PBDEs are three main products at 0.5 hr, and 7Br, 4Br, 5Br, and 6Br PBDEs are four dominant intermediates during 3–12 hr. In other words, the debromination did not follow a stepwise process but go through a multi-electron transfer mechanism, which depressed the formation and accumulation of lower-brominated PBDEs to some extent. In addition, some low molecular weight aliphatic products were detected in the reaction supernatants, which suggested the generated lower-brominated PBDEs (4Br, 3Br) could be oxidized into brominated dienoic acids, and then into shorter chain carboxylic acids (Lei et al., 2014, 2018b). The results further confirmed that the complete debromination only occurred in a consecutive reduction and oxidation system rather than single reduction system through electron transfer process (Lei et al., 2018b).

Surface modifications of TiO_2 many change the degradation intermediates and their distributions. For example, more PBDEs isomers could be identified as the intermediates of BDE209 by replacing the photocatalysts from naked TiO_2 to Pd-TiO_2 composites. In this sense, the photocatalytic debromination showed a low position selectivity on Pd-TiO_2 than on the pristine TiO_2 surface (Li et al., 2014). According to the work of Li et al. (2014), the lack of position selectivity on Pd-TiO_2 is attributed to the co-catalytic effect of Pd, which makes the cleavage of the C-Br bond at every position of the PBDEs occur at comparable rates, and consequently the

lower-brominated PBDEs such as BDE15 could be rapidly debrominated to generate DE. Similarly, complete debromination of BDE47 was achieved over Pd/g-C_3N_4 composites under an illumination of visible light. The *para*-position bromine atoms were found to be more susceptible to debromination than those at *ortho*-positions in the initial stage, implying that the hydro-dehalogenation reaction rather than electron-transfer process was the rate-determining step due to that the *para*-substituted bromine atoms exhibited the least steric hindrance. Particularly, the other bromine-free product except DE was observed, which was identified as DF, which suggested that the Pd atoms may directly engage in C-Br bond cleavage via oxidative addition. This kind of Pd-catalyzed reaction pathways included not only stepwise debromination but also cyclization arising from C-C bond formation at the *ortho*-position of diphenyl ether (Lei et al., 2020b).

Moreover, the *ortho*-position and *para*-position bromine atoms of BDE47 could be released with the less selectivity in some cases. For example, 2,4,4'-tribromodiphenyl ether (BDE28) and 2,2,4'-tribromodiphenyl ether (BDE17) were the dominant products of BDE47 over Ni/g-C_3N_4 with a 3:1 ratio of BDE17 to BDE28. In the system, multiple C-Br bond activation pathways, i.e., outer/inner sphere single electron transfer, nucleophilic attack by hydride, or oxidative addition, may be occurred in photocatalytic system at the same time (Wei et al., 2019). But there is no PBDF or DF observed, which may be ascribed to the relatively weaker affinity of Ni to Br atoms than Pd.

In summary, the photocatalytic reduction could yield the efficient debromination of PBDEs: the higher-brominated PBDEs was rapidly transformed to lower-brominated PBDEs through an electron-transfer process, but the complete debromination should be combined with a subsequent oxidation process; however, the hydrogenation debromination process induced by active hydrogen atoms would be more beneficial to the deep debromination of PBDEs.

1.3. *Electrocatalytic debromination of PBDEs*

A few of investigations have been published on electrocatalytic reduction of PBDEs (Bonin et al., 2005; Konstantinov et al., 2008; Peverly et al., 2013; Su et al., 2012; Liu et al., 2014). Bonin et al. conduct the electrocatalytic degradation of PBDEs with reticulated glassy carbon and IrO_2/Ti as the cathode and anode for the first time (Bonin et al., 2005). At a current of 0.065 A, 75% of BDE15 was converted to BDE3 and DE after 90 min, and the debromination efficiency was evaluated to be 60%. Konstantinov and his co-workers investigated the electrochemical debromination of BDE209 at an inert (Pt) electrode in a mixture of THF and water (Konstantinov et al., 2008). The initial electron transfer and subsequent proton transfer from solvent were confirmed as the rate-determining step. The possible debromination mechanism may be expressed that electrons attack PBDEs to produce free radical anion $ArBr^{\bullet-}$ as a discrete intermediate. The followed steps are divided into two pathways: (1) $ArBr^{\bullet-}$ extracts protons from solvents to form radical complexes, which is followed by dissociation to the reduced product; (2) $ArBr^{\bullet-}$ releases Br^- to obtain the aryl radical Ar•, which subsequently form the product by abstracting hydrogen atoms from solvents (Konstantinov et al., 2008). Therefore, it is essential to select appropriate solvents to improve the electrocatalytic performance. For example, Peverly et al. conducted the electrocatalytic reduction of BDE209 at silver cathode in DMF and DMSO, and found that DMF is more suitable than DMSO (Peverly et al., 2013).

Three cathodic peaks appeared (E_{pc} = -1.46, -1.83 and -2.52 V vs SCE) in the cyclic voltammogram for the reduction of BDE209 on the Ag cathode (Peverly et al., 2013), being attributable to cleavage of C-Br bond of BDE209 and its degradation intermediates. These cathodic peaks and their negative potential shift suggest that the degradation of PBDEs needs relatively negative potential, and the reduction of the lower-brominated intermediates requires much more negative potentials. However, the hydrogen evolution reaction is always considered to be a competitive reaction to limit the degradation efficiency at a negative potential. Therefore, the electrode materials for the electrocatalytic reduction should possess a much high hydrogen evolution overpotential to inhibit the hydrogen evolution reaction as soon as possible. Su et al. selected TiN film as the cathode to carry out electrocatalytic reduction of BDE47 in methanol/water (V/V =7:3) with a degradation constant of BDE47 of 0.65 hr^{-1}, which is 2, 4, 17 times than those on Pt film (0.32 hr^{-1}), Pt wafer (0.16 hr^{-1}) and graphite cathode (0.039 hr^{-1}), respectively (Su et al., 2012). Compared to Pt wafer (-0.12 V vs SCE) and Pt film (-0.07 V vs SCE), the TiN film shows the lowest hydrogen evolution potential of -0.54 V vs SCE. Similarly, Liu and his co-workers report a novel vertically aligned nitrogen-doped nanodiamond (VA-NDD)/Si rod array (RA) electrode with a much lower hydrogen evolution potential (−1.95 V vs Hg/ Hg_2SO_4). Over 97% of BDE47 is electrochemically reduced by using VA-NDD/Si RA Electrode within 2 hr at -1.85 V with a first-order kinetic constant of 1.93 hr^{-1}, which is 8.7, 4.7 3.5 and 2.3 times of those with boron-doped diamond (BDD)/Si RA (0.23 hr^{-1}), graphite (0.41 hr^{-1}), Pt (0.55 hr^{-1}) and Pd (0.85 hr^{-1}) as electrodes (Liu et al., 2014). In addition, the interaction between electrode and PBDEs plays an important on the electrocatalytic reduction of PBDEs. Peverly et al. found that BDE209 gives rise to a cathodic peak at a silver cathode with a much large current than that with a glassy carbon electrode, which demonstrates the ability of silver to promote the cleavage of C-Br bond (Peverly et al., 2013).

Generally, the debromination of BDE47 occurred both on the *ortho*-position and the *para*-position in the abovementioned systems to produce BDE28 and BDE17. Subsequently, the tri-BDEs are debrominated to Di-BDEs including BDE 15 and BDE8, which can be all transformed to BDE3 then to DE (Su et al., 2012; Liu et al., 2014). Compared with the higher-brominated PBDEs, the lower-brominated PBDEs, especially BDE3, are found to be more difficult to be reduced (Su et al., 2012), which is in accord with the mechanism that the electron transfer is the initial step.

As we know, PBDEs have relatively low solubility in water, and the use of more organic solvents for the dissolving the PBDEs is unfavorable for an electrochemical process. In addition, the reduction of PBDEs requires much more negative potentials, under which a large amount of hydrogen bubbles is formed, and vigorous bubbling is unfavorable to the absorption and degradation of PBDEs on the cathode. These may be

important reasons for the limited investigations on the electrocatalytic reduction of PBDEs.

1.4. *Debromination of PBDEs by using zero-valent metal*

In principle, zero-valent active metals can release electrons and yield the reduction of brominated organic substances. Several metals have been investigated for the treatment of polyhalogenated aromatic compounds such as polychlorinated biphenyl, polychlorinated dibenzo-p-dioxins, halogenated phenols, and PBDEs (Garbou et al., 2019; Keum et al., 2005; Li et al., 2021; Yu et al., 2016; Fu et al., 2014).

The debromination of PBDE by using zero-valent metals follows a general electron attacking reductive debromination mechanism, where the zero-valent metal produces electrons and the solvent functions as the hydrogen donor (Yao et al., 2021). However, this major course is possibly mixed with other secondary reactions. By taking zero-valent iron as the example, the dehalogenation of halogenated organic pollutants by zero-valent metal may be described by three general pathways: (1) Fe^0 is directly corroded and the reduction occurs by electron transfer from the Fe^0 surface to the adsorbed halogenated molecules; (2) the in situ generated Fe^{2+} from the corrosion of Fe functions as a reductant capable of causing dehalogenation of halogenated molecules; (3) the hydrogen is produced as a product of corrosion with water and then the hydrogen is activated to form active hydrogen species to contribute to the dehalogenation reaction in the presence of effective catalysts (Matheson et al., 1994).

1.4.1. *Zero-valent iron induced debromination*

By using zero-valent iron, Keum et al. conducted the degradation of PBDEs substituted with 1 to 10 bromine atoms, and found that 92% of BDE209 was converted into lower-brominated PBDEs within 40 days (Keum et al., 2005). The initial reaction rate constant showed positive correlation with the LUMO level or heat of formation, implying that the reduction by zero-valent iron may occur through direct electron transfer and subsequent hydrogenation by reacting with solvents (Zhuang et al., 2010). Later investigates demonstrated that the loading of co-catalysts such as Ag, Pb and Cu significantly enhanced the degradation of PBDEs (Luo et al., 2012; Li et al., 2018; Liang et al., 2014; Wang et al., 2018a; Zheng et al., 2019). Luo et al. reported that about 97% of BDE209 or 78% of BDE47 were reduced to lower-brominated PBDEs within 8 min by Fe-Ag nanoparticles under microwave radiation, because the loaded Ag could alter the electronic properties of iron and enhance the rate of iron corrosion by forming a galvanic couple with Fe (Luo et al., 2012). Moreover, the enhancement of the degradation of PBDEs by loading Ag was also attributed to that the plated Ag accelerates the electron-transfer in Fe/Ag system (Zheng et al., 2019). Wei et al. used the sulfurized nanoscale zerovalent iron (S-nZVI) to remove Pb^{2+} and PBDEs, and found that the generated Pb/Fe in situ accelerated the degradation of PBDEs due to the similar galvanic effect (Wei et al., 2021). Li et al. investigated the debromination of BDE-47 by Cu/Fe^0 in different protic solvents, and found that the debromination efficiency of BDE47 in water by Cu/Fe^0 was about 80% and the contact potential difference of Cu/Fe° contributed to the obvious degradation of BDE47 in deoxygenated water because the electron transfer was the main mechanism for BDE47 degradation by Cu/Fe^0 (Li et al., 2018).

Besides the direct electron transfer from zero-valent iron to PBDEs, the hydrogenation process also occurs in some zero-valent iron systems: hydrogen is produced as a product of corrosion (Matheson et al., 1994), which functions as the reductants for the reductive debromination of PBDEs by the activation of co-catalysts such as Ni and Pd. For example, the degradation rate constant of BDE209 in THF-H_2O (V:V = 50:50) mixture was increased from 0.0042 min^{-1} for zero-valent iron to 0.051 min^{-1} for Ni/Fe bimetallic material, which is due to that the introduction of Ni into Fe accelerated the generation of highly active hydrogen atoms (Tan et al., 2016). By comparing the degradation of lower brominated PBDEs and higher brominated PBDEs, the atomic hydrogen generation of Ni/Fe bimetal was indicated to play an important role in the degradation of PBDEs, especially in lower brominated PBDEs such as BDE47 (Wei et al., 2021). Because of the strong enhancing effect of the Pd introduction, many studies have been focused on the investigation of bimetallic Pd/Fe for the debromination of PBDEs (Huang et al., 2018; Li et al., 2018; Wang et al., 2018a, 2017b, 2019a; Zhuang et al., 2011). Compared to the Ag/Fe and Cu/Fe materials, the debromination of PBDEs becomes much easier by Pd/Fe (Li et al., 2018; Wang et al., 2018a). For example, more than 60% of BDE47 was debrominated to lower-brominated congeners within 6 hr by Pd/Fe in ethanol, but the Cu/Fe particles showed little activity to BDE47 and no formation of lower-brominated products (Li et al., 2018). Zhuang et al. (2011) used E_{LUMO} and heat of formation (H_f) as descriptor variables to correlate with degradation rate constant of PBDEs with 1-3 bromine atoms by Pd/Fe and Fe and found that the linear fittings for Pd/Fe have much lower R^2 values (0.129 for H_f and 0.128 for E_{LUMO}) than for Fe (0.854 for H_f and 0.692 for E_{LUMO}), indicating that the electron transfer is not the rate-determining step in Pd/Fe system (Li et al., 2018). Wang et al. further indicated that the H-atom species adsorbed on the surface of palladium contributed to the enhance reaction rates. Unlike the PBDE debromination by zero-valent iron through electron-transfer process, the degradation rate constants by Pd/Fe was observed to be slightly decreased as the number of bromines was decreased (Li et al., 2018). This suggests that the participation of active hydrogen atoms greatly reduce the accumulation of lower-brominated PBDEs.

1.4.2. *Zero-valent zinc induced debromination*

As a metal, Zn is more active than Fe. Recently, the use of zero-valent zinc has been also investigated for the reductive debromination of PBDEs. Tang et al. (2018) found that the reactivity of zero-valent zinc to BDE47 is much higher than the zero-valent iron , the use of zero-valent zinc reduced 98.3% of BDE47 within 48 hr with the generation of lower-brominated PBDEs. The mechanism of the degradation of PBDEs by zero-valent zinc seems to be similar to the zero-valent iron system. The reaction rates of PBDEs shows a good correlation with E_{LUMO}, suggesting that direct electron transfer between zero-valent zinc and PBDEs is recognized as the major reaction mechanism (Tang et al., 2018). In order to enhance the activity of zero-valent zinc and reduce the accumulation of lower-brominated PBDEs, noble metal Pd was chosen as the co-catalysts due to its high reactivity to convert hydrogen gas

to active hydrogen atoms, which play an important role to enhance the debromination of PBDEs. Xu et al. (2020) reported that more than 97% of BDE47 was degraded by Pd/Zn particles within 2 hr, whereas the Zn particles alone only yielded a degradation efficiency of 65% .

1.4.3. *Products and pathways in zero-valent metal system*

Galvanic corrosion provides the driving force for the degradation of BDE47 and its reductive intermediates, and the debromination proceeds by the electron transfer process. The stepwise debromination of PBDEs is still the major pattern of debromination in zero-valent metal systems. The *ortho*-position bromine atoms of PBDEs are preferentially released (Keum et al., 2005; Li et al., 2018; Tang et al., 2018; Wang et al., 2018a; Zhuang et al., 2010; Zheng et al., 2019). For example, a preference for *ortho*-debromination of BDE47 was displayed by Cu/Fe in water with the accumulation of *para*-substituted brominated products: the concentration of BDE28, BDE15 (4,4'-dibromodiphenyl ether) and BDE3 (4-monobromodiphenyl) exceeded the corresponding BDE 17, BDE4 (2,2'-dibromodiphenyl ether) and BDE1 (2-monobromodiphenyl ether) (Li et al., 2018). On the contrary, a preference for *para*-debromination of BDE47 and lower-brominated PBDEs was observed by Ni-modified or Pd modified zero-valent system, and the position-selectivity was mainly influenced by steric hindrances between Br and Br or O of PBDEs, which is attributed to the prominent role of active hydrogen atom. The distance between neighboring bromines, between *ortho*-bromine atom and the bridging oxygen atom are evaluated to be about 3.1–3.4 Å and 3.0–3.2 Å, respectively (Li et al., 2018). However, the diameter of H atom is too large (about 1.06 Å) to attack the *ortho*-position bromine, thereby the *para*-position bromine atoms may easily get debrominated as a result of H-atom transfer. Therefore, BDE17, BDE4 and BDE1 were identified as the main intermediates in these systems. In general, the products and pathways in zero-valent metal systems show the similar results as the photocatalytic system.

Moreover, there are two points needed to be emphasized, the one is that, generated as by-products, DF is only produced in the systems containing Pd due to its strong affinity to bromine atom (Li et al., 2018). Secondly, both the electron transfer process and the hydrogenation reaction occur at the same time in a zero-valent metal system, but only one (either the electron transfer process or the hydrogenation reaction) dominates the debromination in other systems.

1.5. *Chemically catalytic reductive debromination of PBDEs with using reducing agent*

According to the above analysis, the hydrogenation rather than electron transfer is more favorable to the complete and rapid debromination of PBDEs under mild conditions. Therefore, some strategies about chemically catalytic reductive debromination, especially catalytic transfer hydrogenation (CTH) systems, have been proposed for the reduction of PBDEs (Lei et al., 2020a, 2018a; Ukisu et al., 2015). CTH draw a lot of attention due to its advantages of high efficiency, mild reaction in comparison to the traditional catalytic hydrogenation by using H_2 as hydrogen donor. Several hydrogen donors including alcohols, $NaBH_4$, $N_2H_4 \bullet H_2O$, formic acid and so on could be introduced to allow the CTH reaction, while noble metal (Pd, Ru, Rh) and noble-free metal (Cu, Ni) are always used as the catalysts (Lei et al., 2018a).

1.5.1. *Chemically catalytic reductive debromination of PBDEs with alcohols*

Catalytic transfer hydrogenation using alcohols as the hydrogen source over the metals have been widely used for the treatment of halogenated organic pollutants in recent years due to its low costs and environmentally friendly of alcohols. Although the mechanism for the hydrogenation on metal surfaces has not been well clarified, the chemically catalytic debromination processes are always dependent on the used metal. Generally, the required hydrogen transfer via active hydrogen species (hydrogen atom or hydride) is preferred on metals with low hydrogen overpotentials such as Pd, Rh (Baumgartner et al., 2013; Ukisu et al., 1997). whereas on other metals with moderate or high hydrogen overpotentials such as Cu, Ni, Au, both active hydrogen species and electron contributes to the hydro-dehalogenation reactions (Wang et al., 2018b).

In recent years, the investigations for catalytic reductive debromination of PBDEs are focused on the noble metal Pd. For example, Ukisu achieved the complete debromination of BDE209 with silica-supported Pd nanoparticle as catalysts in a solution of 2-propanol/methanol containing dissolved NaOH, leading to two final products, DE and DF, are generated, which indicates that the catalytic reaction may include not only a hydro-debromination by active hydrogen species but also a cyclization reaction by C-C coupling (Ukisu et al., 2015). In order to improve the reaction activity of the catalysts, Lei et al. (2020a) utilized nano-sized Pd/TiO_2 composites with a low Pd content of 1wt% as catalysts to reduce BDE47 in isopropanol containing dissolved NaOH at 40 °C, and the debromination efficiency of BDE47 reaches up to 100% within 60 min . Furthermore, the reaction mechanism is clarified in detail (**Fig. 5**): alcohols are firstly dissociated in NaOH solution, then activated by Pd nanoparticles to produce active hydrogen species. Subsequently, the formed active hydrogen species attack the adsorbed BDE47 molecules, which leads to the hydro-debromination of BDE47. After the stepwise hydro-debromination of BDE47 to generate BDE4, both hydro-debromination and coupling-debromination are occurred on the Pd nanoparticles. The hydro-debromination is induced by hydrogen species to form DE, while the coupling reaction is occurred through two oxidative addition, one reductive dissociation and one reductive elimination to generate DF due to that the strong affinity of Pd to bromine atoms could initiate an Ullmann-type reaction (Lei et al., 2020a).

1.5.2. *Chemically catalytic reductive debromination of PBDEs with other reducing agents*

Except for alcohols, other reducing agents such as $NaBH_4$ and $N_2H_4 \bullet H_2O$ are able to be used as hydrogen donors to conduct a chemically catalytic reductive debromination. Because these reducing compounds have much stronger reducibility and hydrogen donating ability than alcohols, these reducing agents themselves may reduce PBDEs to lower-brominated PBDEs without using catalysts (Granelli et al., 2011). However, if we hope to achieve rapid and complete debromination of

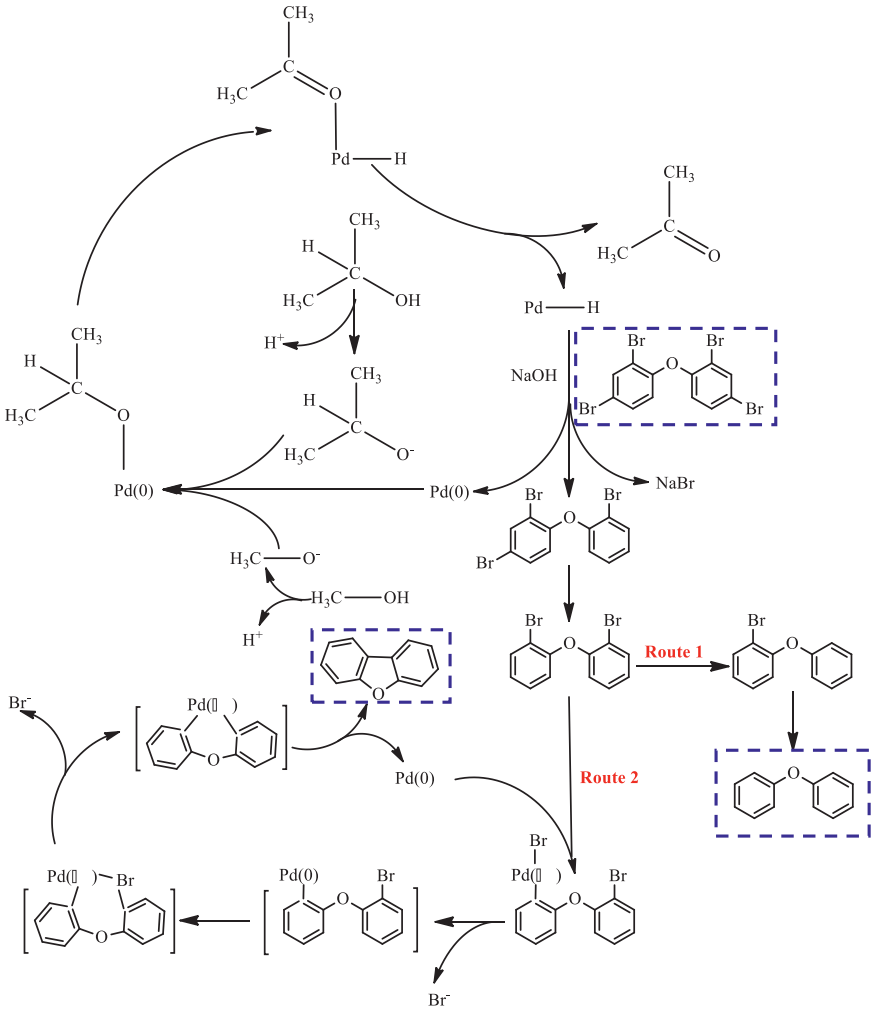

Fig. 5 – Mechanism the reductive debromination of BDE47 on 1%Pd/TiO_2 in a solution of isopropanol containing NaOH at 40 °C (Lei et al., 2020a).

PBDEs on mild conditions, it is necessary to combine the use of reducing agents and suitable catalysts.

Lei et al. (2018a) developed a new method for ultrarapid and deep debromination of BDE47 under mild conditions by using noble-metal-free Cu/TiO_2 catalyst . The simultaneous addition of Cu/TiO_2 and N_2H_4•H_2O yield a drastic increase of the degradation and debromination efficiency to 100% and 87.7% within 3 s, and the complete debromination could be achieved by multiple addition of N_2H_4•H_2O. By increasing the total concentration of N_2H_4•H_2O, all the Br atoms of the added BDE47 at high concentration (e.g., 1500 mg/L) are released as bromine ions (**Fig. 6**) (Lei et al., 2018a). Compared with the abovementioned photolytic, photocatalytic, electrochemical and zero-valent metal reduction systems, this system has at least following merits: no needs for anaerobic atmosphere, no special needs for controlling reaction temperature or extra energy, very short treating time, and very high debromination concentration and depth. Therefore, the chemically catalytic reductive debromination may be the most hopeful technology for the treatment of PBDEs in liquid system.

It was noted that the above Cu/TiO_2-N_2H_4•H_2O system for the complete debromination of BDE47 required a fairly high consumption of the reducing agent N_2H_4•H_2O. In order to decrease the consumption of the reducing agent, Lei et al. (2018a) further developed a Pd^{2+}-N_2H_4•H_2O system, in which the required consumption of the reducing agent N_2H_4•H_2O was able to be decreased by about 20 times (Tang et al., 2022).

1.6. *Mechanochemical reductive debromination of PBDEs*

Mechanochemical method is one that conducted in a solid phase without solvents by grinding co-milling agents and halogenated organic pollutants, in which the mechanical energy is transferred from the ball milling to the solid system to accelerate the chemical reaction. Here, the reducing agents in mechanochemical reduction mainly include hydrides (e.g. CaH_2, $NaBH_4$, $LiAlH_4$) and zero-valent active metals (e.g., Fe, Al, Zn). Because the dehalogenation of chlorinated or fluorinated organic pollutants is more difficult than the debromination of the corresponding brominated organic pollutants, the researches on the mechanochemical reduction have been mainly conducted for the dehalogenation of chlorinated or fluorinated organic pollutants in recent years (Cagnetta et al., 2016; Monagheddu et al., 1999; Lv et al., 2018). All the devel-

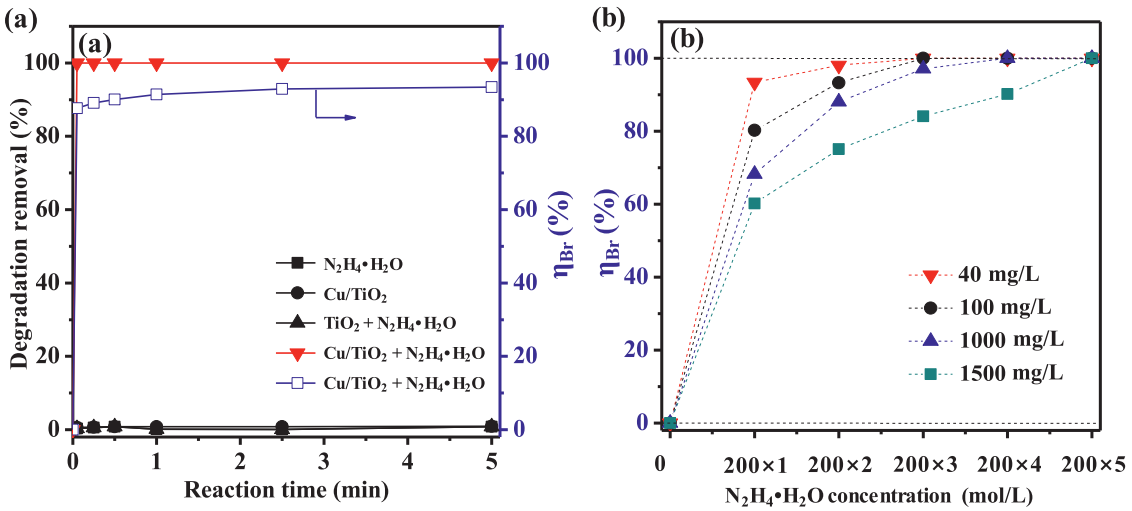

Fig. 6 – (a) Degradation (solid symbols) and debromination efficiency (hollow symbols, η_{Br}) of BDE47 (40 mg/L) in various systems. (b) Effects of multiple additions of $N_2H_4•H_2O$ on the debromination efficiency of BDE47 at different initial concentrations over Cu/TiO_2. In the experiment, the degradation was conducted for 5 min after the first addition of $N_2H_4•H_2O$ (200 × 1 mmol/L). The second run of the degradation was conducted for 5 min by doing the second addition of $N_2H_4•H_2O$ (another 200 mmol/L, and the total addition 200 × 2 mmol/L). The next runs of the addition were similarly labelled (Lei et al., 2018a).

oped mechanochemical reduction systems for the dechlorination of chlorinated organic pollutants, in principle, can be used for the debromination of brominated organic pollutants after a slight modification.

Zhang et al. investigated the degradation of BDE209 by using Fe powder, and found that the removal efficiency was only 24.0% by using Fe alone as grinding agent after ball milling for 30 min and then the further removal was hardly to be observed as prolonging milling time to 2 hr (Zhang et al., 2017). This was attributed to that Fe powders is efficient for the reduction of PBDEs, but the rapid generation of iron oxides resulted in the passivation of Fe milling agent, apparently stopping the BDE209 degradation. Because SiO_2 can inhibit the agglomeration during milling and the cleavage of ≡SiO– chemical bond by ball milling generates silyl≡Si$^{•}$ and siloxyl Si-O≡$^{•}$ radicals being reactive toward organic compounds (Wang et al., 2020). Wang et al. conducted the mechanochemical reduction of waste printed circuit boards (WPCBs) by using the mixture of Fe and SiO_2. However, in this system, the debromination efficiency was 21.8% after ball milling for 12 hr, and under the same conditions, CaO increased the debromination efficiency is as high as 45.1% after 12 hr. After getting that get high surface energy during the ball-milling process, CaO powders functioned as a good electron donor to break the C-Br bond of BDE209, producing lower-brominated PBDEs. The mechanochemical reduction process is not a pure reduction process, but a mixed one of both oxidation and reduction process. Therefore, in addition to the lower-brominated PBDEs, the final degradation products contained also open-ring products, graphite carbon, amorphous and even other products carbon detected in this system. Because the lower-brominated PBDEs are more difficult to be reduced and the electron denoting ability of Fe powders and CaO powders are limited, the main product was BDE118, which seems to favorably be oxidized (Wang et al., 2020). In consideration of the *in situ* coupling of reduction and oxidation processes, Zhang et al. (2017). developed a mixture system of Fe powders and Bi_2O_3 powders as co-milling agents, and achieved the debromination of BDE209 via its rapid reduction over Fe powders and the subsequent oxidation of its dibrominated intermediates over Bi_2O_3. In this system, the degradation efficiency of BDE209 after 2 hr of ball milling was a high as 96.6%, being 4.0 times that in the single Fe system. More importantly, the ratio of covalently bonded bromine atoms to the total bromine only left 15%, and that of the bromine ions was increased to 85% .

In general, the complete debromination of PBDEs by ball-milling proceeds by the reduction and oxidation at the same time rather than the single pure reduction, because the intermediates such as lower-brominated PBDEs is easy to be accumulated in the single reductive system. Most of PBDEs in environment exists in solid phases due to their strong hydrophobicity. Therefore, the mechanochemistry is considered to be one of the most suitable technology for the treatment of PBDEs in environment.

1.7. *A brief comparison between the debromination by various chemical modes*

A brief comparison between the debromination by various chemical modes is tabulated in **Table 2**. These techniques involve the photolytic reduction, photocatalytic reduction, electrocatalytic reduction, zero-valent metal reduction, chemically catalytic reduction and mechanochemical reduction.

In the liquid system, photolytic reduction is always used to evaluate the potential risks of PBDEs in real environment but limited to be applied in their treatment in the real engineering due to that the required light wavelength is too short to make the technique too energy-consuming. Many efforts have been

Table 2 – Comparisons between the debromination of PBDEs in typical reductive processes

Reduction mode	Catalyst	PBDEs (mg/L)	η [a] (reaction time)	Reactive species [b]	Final products	Refs.
Photolysis	none	BDE47 (5)	> 25% (60 min)	e^-	DE, 1- to 3-BDEs	Wang et al. (2017a)
Photolysis	none	BDE209 (none)	> 10% (8 hr)	e^-	4- to 9-BDEs, PBDFs	Söderström et al. (2004)
UV Photocatalysis	TiO_2	BDE209 (10)	~40% (24 hr)	e^-	4- to 7-BDEs	Sun et al. (2009)
UV Photocatalysis	CuO/TiO_2	BDE47 (5)	50% (7.5 min)	e^-	2-BDEs	Lei et al. (2016b)
UV Photocatalysis	Pd/TiO_2	BDE209 (10)	100% (60 min)	H^*	DE	Li et al. (2014)
Vis. Photocatalysis	Ag/CdS	BDE47 (5)	44.3% (30 min)	e^-	1- to 3-BDEs	Wang et al. (2019c)
Vis. Photocatalysis	$Pd/g\text{-}C_3N_4$	BDE47 (5)	100% (2 hr)	H^*	DE, DF	Lei et al. (2020a,2020b)
Electrocatalysis	Carbon	BDE15 (708)	~60% (90 min)	e^-	DE, 1-BDEs	Bonin et al. (2005)
Electrocatalysis	TiN	BDE47 (5)	~70% (5 hr)	e^-	DE, 1- to 3-BDEs	Peverly et al. (2013)
Electrocatalysis	VA-NDD/Si RA	BDE47 (20)	~ 85% (3 hr)	e^-	DE, 1- to 2-BDEs	Liu et al. (2015)
Zero-valent metal	Fe	BDE209 (5)	~55% (40 days)	e^-	2- to 7-BDEs	Keum et al. (2005)
Zero-valent metal	Ag/Fe	BDE47 (5)	~40% (15 min)	e^-	2- to 9-BDEs	Luo et al. (2012)
Zero-valent metal	Pd/Fe	BDE47 (20)	~95% (24 hr)	H^*	DE, DF	Li et al. (2018)
Zero-valent metal	Zn	BDE47 (2.5)	~50% (50 hr)	e^-	2-BDEs	Tang et al. (2018)
Zero-valent metal	Pd/Zn	BDE47 (4.5)	~90% (50 hr)	H^*	DE, 1- to 4-BDEs	Xu et al. (2020)
Chemical catalysis	Pd/SiO_2-45 °C	BDE209 (3000)	100% (2 hr)	H^*	DE, DF	Ukiso et al. (2015)
Chemical catalysis	Pd/TiO_2-40°C	BDE47 (100)	100% (1 hr)	H^*	DE, DF	Lei et al. (2020a)
Chemical catalysis	Cu/TiO_2-$N_2H_4 \bullet H_2O$	BDE47 (1500)	60% (3 sec); 100% (25 min)	H^*	DE	Lei et al. (2018a)
Chemical catalysis	Pd^{2+}-$N_2H_4 \bullet H_2O$	BDE47 (20)	100% (20 min)	H^*	DE, DF	Tang et al. (2022)
Mechanochemistry	Fe-Bi_2O_3	BDE209 (0.278 g)	85% (2 hr)	e^-, O^{2-}	CO_2, H_2O	Zhang et al. (2017)

[a] η is debromination efficiency, and the reaction time is given in the followed parenthesis;
[b] Main reactive species: e^- is electron, and H^* is active hydrogen species;

done for the photocatalytic reduction, electrocatalytic reduction and zero-valent metal reduction of PBDEs, especially photocatalytic reduction and zero-valent metal reduction are the most widely reported in the literatures. Nevertheless, most of these techniques could reduce higher-brominated PBDEs but lead to the accumulation of lower-brominated PBDEs, because lower-brominated PBDEs have much slower degradation rates than higher-brominated PBDEs in the electron-transfer process. It is worth noting that the complete debromination of PBDEs is relatively easy to be achieved by the introduction of noble metal Pd owing to its strong affinity to Br atoms and easily generation of active hydrogen species. Chemically catalytic reduction with alcohols or reducing agents as hydrogen donors is considered as the promising technique for the rapid and complete debromination of PBDEs at high concentrations. In addition, mechanochemical reduction can be used to the treatment of PBDEs in solid phase. PBDEs can be transformed to graphite carbon or amorphous carbon finally by mall-billing, which is environmentally friendly. The related literatures for the mechanochemical reduction of PBDEs are limited, and the difficulty is to select suitable co-milling agents to increase the debromination efficiency and decrease the energy consumption.

2. Conclusions and perspectives

In this review, a summary of current advances in chemical reduction for the treatment of PBDEs has been proposed including photolysis, photocatalysis, electrocatalysis, zero-valent metal reduction, chemically catalytic reduction and mechanochemical method. Among the chemical reductive methods, the hydrogenation debromination rather than an electron-transfer route seems to be the most suitable for the rapid and complete debromination of PBDEs at high concentration in liquid system, while the mechanochemical reduction is favorable for the PBDEs in the solid matrix. To facilitate the practical application of the two techniques in field of en-

vironmental engineering, some suspects and challenges need to be further investigated.

Firstly, in the hydrogenation debromination process, the active hydrogen species provided by hydrogen donors prefers to be generated over the noble metals such as Pd, Ru and Rh, but the reducing agents is needed and the utilization of reducing agents is too low on the surface of noble-free metals. Therefore, it is essential to design an excellent system based on the noble-free metals with high efficiency for the activation of the hydrogen donors to produce active hydrogen species.

Secondly, the interaction between catalysts and hydrogen donors have been confirmed to play an important role on the debromination behavior of PBDEs, but the other interaction including catalysts and pollutants, catalysts and solvents, pollutants and hydrogen donors and so on should be systematically investigated in the future.

Thirdly, most of the catalysts used for the reductive debromination of PBDEs are nano-sized and require a careful preparation process in specific conditions. On one hand, the tedious operation goes against its application in the real engineering; On the other hand, the nanocatalysts may produce secondary pollution, thus its potential risk should be evaluated and considered by the researchers.

At last, the mechanochemical methods are suitable to treat the PBDEs in the solid phase, whereas the investigations about mechanochemical reduction of PBDEs are limited, and the reducing agents used as co-milling agents showed a relatively low efficiency for the treatment of PBDEs, especially PBDEs in the real waste printed circuit boards. So, it is necessary to explore more excellent co-milling agents to enhance its debromination performance and decrease the energy-consuming in the ball-milling process.

Declaration of Competing Interest

The authors declare that they have no known competing financial interests or personal relationships that could have appeared to influence the work reported in this paper.

Acknowledgments

This work was supported by the National Natural Science Foundation of China (Nos. 21707170, 21777194 and 22076052), the Natural Science Foundation of Hubei Province (No. 2021CFB535), the Fundamental Research Funds for the Central Universities of South-Central MinZu University (No. CZT20019).

REFERENCES

Abbasi, G., Buser, A.M., Soehl, A., Murray, M.W., Diamond, M.L., 2015. Stocks and flows of PBDEs in products from use to waste in the U.S. and Canada from 1970 to 2020. Environ. Sci. Technol. 49, 1521–1528.

Abbasi, G., Li, L., Breivik, K., 2019. Global historical stocks and emissions of PBDEs. Environ. Sci. Technol. 53, 6330–6340.

Abdullah, H., Khan, M.R., Ong, H.R., Yaakob, Z., 2017. Modified TiO_2 photocatalyst for CO_2 photocatalytic reduction: an overview. J. CO_2 Util. 22, 15–32.

Ahmed, S.F., Mofijur, M., Nuzhat, S., Chowdhury, A.T., Rafa, N., Alhaz Uddin, M., et al., 2021. Recent developments in physical, biological, chemical, and hybrid treatment techniques for removing emerging contaminants from wastewater. J. Hazard. Mater. 416, 125912.

Baumgartner, R., Stieger, G.K., McNeill, K., 2013. Complete hydrodehalogenation of polyfluorinated and other polyhalogenated benzenes under mild catalytic conditions. Environ. Sci. Technol. 47, 6545–6553.

Besis, A., Samara, C., 2012. Polybrominated diphenyl ethers (PBDEs) in the indoor and outdoor environments-a review on occurrence and human exposure. Environ. Pollut. 169, 217–229.

Bonin, P.M., Edwards, P., Bejan, D., Lo, C.C., Bunce, N.J., Konstantinov, A.D., 2005. Catalytic and electrocatalytic hydrogenolysis of brominated diphenyl ethers. Chemosphere 58, 961–967.

Cagnetta, G., Robertson, J., Huang, J., Zhang, K., Yu, G., 2016. Mechanochemical destruction of halogenated organic pollutants: a critical review. J. Hazard. Mater. 313, 85–102.

Chen, K., Wang, X., Xia, P., Xie, J., Wang, J., Li, X., et al., 2020. Efficient removal of 2,2',4,4'-tetrabromodiphenyl ether with a Z-scheme Cu_2O-(rGO-TiO_2) photocatalyst under sunlight irradiation. Chemosphere 254, 126806.

Currier, H., Fremlin, K., Elliott, J., Drouillard, K., Williams, T., 2020. Bioaccumulation and biomagnification of PBDEs in a terrestrial food chain at an urban landfill. Chemosphere 238, 124577.

De Wit, C.A., 2002. An overview of brominated flame retardants in the environment. Chemosphere 46, 583–624.

Eriksson, J., Green, N., Marsh, G., Bergman, Å., 2004. Photochemical decomposition of 15 polybrominated diphenyl ether congeners in methanol/water. Environ. Sci. Technol. 38, 3119–3125.

Fu, F., Dionysiou, D.D., Liu, H., 2014. The use of zero-valent iron for groundwater remediation and wastewater treatment: a review. J. Hazard. Mater. 267, 194–205.

Gallen, C., Drage, D., Kaserzon, S., Baduel, C., Gallen, M., Banks, A., et al., 2016. Occurrence and distribution of brominated flame retardants and perfluoroalkyl substances in Australian landfill leachate and biosolids. J. Hazard. Mater. 312, 55–64.

Garbou, A.M., Liu, M., Zou, S., Yestrebsky, C.L., 2019. Degradation kinetics of hexachlorobenzene over zero-valent magnesium/graphite in protic solvent system and modeling of degradation pathways using density functional theory. Chemosphere 222, 195–204.

Granelli, L., Eriksson, J., Bergman, Å., 2012. Sodium borohydride reduction of individual polybrominated diphenyl ethers. Chemosphere 86, 1008–1012.

Granelli, L., Eriksson, J., Athanasiadou, M., Bergman, Å., 2011. Reductive debromination of nonabrominated diphenyl ethers by sodium borohydride and identification of octabrominated diphenyl ether products. Chemosphere 82, 839–846.

Guo, S., Zhu, L., Majima, T., Lei, M., Tang, H., 2019. Reductive debromination of polybrominated diphenyl ethers: dependence on Br number of the Br-rich phenyl ring. Environ. Sci. Technol. 53, 4433–4439.

Harrad, S., Drage, D., Sharkey, M., Berresheim, H., 2019. Brominated flame retardants and perfluoroalkyl substances in landfill leachate from Ireland. Sci. Total Environ. 695, 133810.

Hu, J., Eriksson, L., Bergman, Å., Jakobsson, E., Kolehmainen, E., Knuutinen, J., et al., 2005. Molecular orbital studies on brominated diphenyl ethers. Part II-reactivity and quantitative structure- activity (property) relationships. Chemosphere 59, 1043–1057.

Hu, Z., Wang, X., Dong, H., Li, S., Li, X., Li, L., 2017. Efficient photocatalytic degradation of tetrabromodiphenyl ethers and

simultaneous hydrogen production by TiO_2-Cu_2O composite films in N_2 atmosphere: influencing factors, kinetics and mechanism. J. Hazard. Mater. 340, 1–15.
Hua, I., Kang, N., Jafvert, C., Fábrega-duque, J., 2003. Heterogeneous photochemical reactions of decabromodiphenyl ether. Environ. Chem. 22, 798–804.
Huang, A., Wang, N., Lei, M., Zhu, L., Zhang, Y., Lin, Z., et al., 2013. Efficient oxidative debromination of decabromodiphenyl ether by TiO_2-mediated photocatalysis in aqueous environment. Environ. Sci. Technol. 47, 518–525.
Huang, C., Zeng, Y., Luo, X., Ren, Z., Tang, B., Lu, Q., et al., 2019. *In situ* microbial degradation of PBDEs in sediments from an e-waste site as revealed by positive matrix factorization and compound-specific stable carbon isotope analysis. Environ. Sci. Technol. 53, 1928–1936.
Huang, G., Wang, M., Hu, Y., Cheng, J., Lv, S., Yang, K., 2018. Reductive degradation of 2,2',4,4'-tetrabromodiphenyl ether with PAC-Pd/Fe nanoparticles: effects of Pd loading, initial pH and HA, and degradation pathway. Chem. Eng. J. 334, 1252–1259.
Huang, K., Lu, G., Lian, W., Xu, Y., Wang, R., Tang, T., et al., 2017. Photodegradation of 4,4-debrominated diphenyl ether in Triton X-100 micellar solution. Chemosphere 180, 423–429.
Keum, Y., Li, Q., 2005. Reductive debromination of polybrominated diphenyl ethers by zerovalent iron. Environ. Sci. Technol. 39, 2280–2286.
Konstantinov, A., Bejan, D., Bunce, N.J., Chittim, B., McCrindle, R., Potter, D., et al., 2008. Electrolytic debromination of PBDEs in DE-83TM technical decabromodiphenyl ether. Chemosphere 72, 1159–1162.
Lei, M., Guo, S., Wang, Z., Zhu, L., Tang, H., 2018a. Ultrarapid and deep debromination of tetrabromodiphenyl ether over noble-metal-free Cu/TiO_2 nanocomposites under mild conditions. Environ., Sci. Technol. 52, 11743–11751.
Lei, M., Wang, N., Guo, S., Zhu, L., Ding, Y., Tang, H., 2018b. A one-pot consecutive photocatalytic reduction and oxidation system for complete debromination of tetrabromodiphenyl ether. Chem. Eng. J. 345, 586–593.
Lei, M., Wang, N., Zhu, L., Xie, C., Tang, H., 2014. A peculiar mechanism for the photocatalytic reduction of decabromodiphenyl ether over reduced graphene oxide-TiO_2 photocatalyst. Chem. Eng. J. 241, 207–215.
Lei, M., Wang, N., Zhu, L., Tang, H., 2016a. Peculiar and rapid photocatalytic degradation of tetrabromodiphenyl ethers over Ag/TiO_2 induced by interaction between silver nanoparticles and bromine atoms in the target. Chemosphere 150, 536–544.
Lei, M., Wang, N., Zhu, L., Zhou, Q., Nie, G., Tang, H., 2016b. Photocatalytic reductive degradation of polybrominated diphenyl ethers on CuO/TiO_2 nanocomposites: a mechanism based on the switching of photocatalytic reduction potential being controlled by the valence state of copper. Appl. Catal. B Environ. 182, 414–423.
Lei, M., Wang, Z., Tang, Y., Wang, H., Zhu, L., Tang, H., 2020a. Peculiar and full debromination of tetrabromodiphenyl ether on Pd/TiO_2: a competing route through hydro-debromination and coupling-debromination. Appl. Catal. B Environ. 275, 119093.
Lei, M., Wang, Z., Zhu, L., Nie, W., Tang, H., 2020b. Complete debromination of 2,2',4,4'-tetrabromodiphenyl ether by visible-light photocatalysis on g-C_3N_4 supported Pd. Appl. Catal. B Environ. 261, 118236.
Li, H., Wang, J., Wang, R., Huang, K., Luo, W., Tao, X., et al., 2018. Debromination of 2,2',4,4'-tetrabromodiphenyl ether (BDE-47) by synthetic Pd/Fe^0 and Cu/Fe^0 in different protic solvents. Chemosphere 212, 946–953.
Li, L., Chang, W., Wang, Y., Ji, H., Chen, C., Ma, W., et al., 2014. Rapid, photocatalytic and deep debromination of polybrominated diphenyl ethers on Pd-TiO_2: intermediates and pathways. Chem. Eur. J. 20, 11163–11170.
Li, N., Wang, B., Si, Y., Xue, F., Zhou, J., Lu, Y., et al., 2019. Toward high-value hydrocarbon generation by photocatalytic reduction of CO_2 in water vapor. ACS Catal. 9 (6), 5590–5602.
Li, Y., Zhao, H., Zhu, L., 2021. Remediation of soil contaminated with organic compounds by nanoscale zero-valent iron: a review. Sci. Total Environ. 760, 143413.
Linsebigler, A.L., Lu, G., Yates, J.T., 1995. Photocatalysis on TiO_2 surfaces: principles, mechanisms, and selected results. Chem. Rev. 95, 735–758.
Liang, D., Yang, Y., Xu, W., Peng, S., Lu, S., Xiang, Y., 2014. Nonionic surfactant greatly enhances the reductive debromination of polybrominated diphenyl ethers by nanoscale zero-valent iron: mechanism and kinetics. J. Hazard. Mater. 278, 592–596.
Liu, H., Tang, S., Zheng, X., Zhu, Y., Ma, Z., Liu, C., et al., 2015. Bioaccumulation, biotransformation, and toxicity of BDE-47, 6-OH-BDE-47, and 6-MeO-BDE47 in early life-stages of zebrafish (*daniorerio*). Environ. Sci. Technol. 49, 1823–1833.
Liu, Y., Chen, S., Quan, X., Fan, X., Zhao, H., Zhao, Q., et al., 2014. Nitrogen-doped nanodiamond rod array electrode with superior performance for electroreductive debromination of polybrominated. Appl. Catal. B Environ. 154-155, 206–212.
Luo, S., Yang, S., Sun, C., Gu, J., 2012. Improved debromination of polybrominated diphenyl ethers by bimetallic iron-silver nanoparticles coupled with microwave energy. Sci. Total Environ. 429, 300–308.
Lv, H., Wang, N., Zhu, L., Zhou, Y., Li, W., Tang, H., 2018. Alumina-mediated mechanochemical method for simultaneously degrading perfluorooctanoic acid and synthesizing a polyfluoroalkene. Green Chem. 20, 2526–2533.
Lv, Y., Cao, X., Jiang, H., Song, W., Chen, C., Zhao, J., 2016. Rapid photocatalytic debromination on TiO_2 with in-situ formed copper co-catalyst: enhanced adsorption and visible light activity. Appl. Catal. B Environ. 194, 150–156.
Matheson, L.J., Tratnyek, P.G., 1994. Reductive dehalogenation of chlorinated methanes by iron metal. Environ. Sci. Technol. 28, 2045–2053.
Miller, E.B., Zahran, E.M., Knecht, M.R., Bachas, L.G., 2017. Metal oxide semiconductor nanomaterial for reductive debromination: visible light degradation of polybrominated diphenyl ethers by Cu_2O@Pd nanostructures. Appl. Catal. B Environ. 213, 147–154.
Monagheddu, M., Mulas, G., Doppiu, S., Cocco, G., Raccanelli, S., 1999. Reduction of polychlorinated dibenzodioxins and dibenzofurans in contaminated muds by mechanically induced combustion reactions. Environ. Sci. Technol. 33, 2485–2488.
Nguyen, V., Smith, S.M., Wantala, K., Kajitvichyanukul, P., 2020. Photocatalytic remediation of persistent organic pollutants (POPs): a review. Arab. J. Chem. 13, 8309–8337.
Pan, Y., Chen, J., Zhou, H., Cheung, S.G., Tam, N.Y., 2019. Degradation of BDE-47 in mangrove sediments under alternating anaerobic-aerobic conditions. J. Hazard. Mater. 378, 120709.
Peverly, A.A., Pasciak, E.M., Strawsine, L.M., Wagoner, E.R., Peters, D.G., 2013. Electrochemical reduction of decabromodiphenyl ether at carbon and silver cathodes in dimethylformamide and dimethyl sulfoxide. J. Electroanal. Chem. 704, 227–232.
Santos, M.F., Alves, A., Madeira, L., 2016. Chemical and photochemical degradation of polybrominated diphenyl ethers in liquid systems- a review. Water Res. 88, 39–59.
Shan, A., Li, M., Li, X., Li, Y., Yan, M., Xian, P., et al., 2019. BDE-47 decreases progesterone levels in bewo cells by interfering with mitochondrial functions and genes related to cholesterol transport. Chem. Res. Toxicol. 32, 621–628.

Shao, Y., Ye, W., Sun, C., Liu, C., Wang, Q., 2017. Visible-light-induced degradation of polybrominated diphenyl ethers with AgI-TiO_2. RSC Adv. 7, 39089–39095.

Shao, Y., Ye, W., Sun, C., Liu, C., Wang, Q., Chen, C., et al., 2018. Enhanced photoreduction degradation of polybromodiphenyl ethers with Fe_3O_4-g-C_3N_4 under visible light irradiation. RSC Adv. 8 (57), 10914–10921.

Sheng, G., Shao, Y., Ye, W., Sun, C., Chen, C., Crittenden, J.C., et al., 2018. Weak-bond-based photoreduction of polybrominated diphenyl ethers on graphene in water. ACS Sustain. Chem. Eng. 6, 6711–6717.

Shi, J., Qu, R., Feng, M., 2015. Oxidative degradation of decabromodiphenyl ether (BDE209) by potassium permanganate: reaction pathways, kinetics, and mechanisms assisted by density functional theory calculations. Environ. Sci. Technol. 49, 4209–4217.

Söderström, G., Sellström, U., De Wit, C.A., Tysklind, M., 2004. Photolytic debromination of decabromodiphenyl ether (BDE209). Environ. Sci. Technol. 38, 127–132.

Su, J., Lu, N., Zhao, J., Yu, H., Huang, H., Dong, X., et al., 2012. Nano-cubic structured titanium nitride particle films as cathodes for the effective electrocatalytic debromination of BDE-47. J. Hazard. Mater. 231-232, 105–113.

Sun, C., Zhao, D., Chen, C., Ma, W., Zhao, J., 2009. TiO_2-mediated photocatalytic debromination of decabromodiphenyl ether: kinetics and intermediates. Environ. Sci. Technol. 43, 157–162.

Tan, L., Liang, B., Cheng, W., Fang, Z., Tsang, E.P., 2016. Effect of solvent on debromination of decabromodiphenyl ether by Ni/Fe nanoparticles and nano zero-valent iron particles. Environ. Sci. Pollut. Res. 23, 22172–22182.

Tang, T., Lu, G., Wang, R., Chen, H., Fang, Y., Huang, K., et al., 2018. Debromination of polybrominated diphenyl ethers (PBDEs) by zero valent zinc: Mechanisms and predicting descriptors. J. Hazard. Mater. 352, 165–171.

Tang, Y., Zhou, X., Lei, M., Wang, H., Lu, A., Zhang, G., et al., 2022. Highly efficient catalytic debromination of tetrabromodiphenyl ether with hydrazine as reducing agent: the role of the interaction between the catalyst and the reducing agent. Chem. Eng. J. 433, 134364.

Tao, F., Sellström, U., De Wit, C.A., 2019. Organohalogenated flame retardants and organophosphate esters in office air and dust from Sweden. Environ. Sci. Technol. 53, 2124–2133.

Ti, Q., Gu, C., Cai, J., Fan, X., Zhang, Y., Bian, Y., et al., 2020. Understanding the role of bacterial cellular adsorption, accumulation and bioavailability regulation by biosurfactant in affecting biodegradation efficacy of polybrominated diphenyl ethers. J. Hazard. Mater. 393, 122382.

Tongue, A.W., Reynolds, S.J., Fernie, K., Harrad, S., 2019. Flame retardant concentrations and profiles in wild birds associated with landfill: a critical review. Environ. Pollut. 248, 646–658.

Tugaoen, H., Herckes, P., Hristovski, K., Westerhoff, P., 2018. Influence of ultraviolet wavelengths on kinetics and selectivity for N-gases during TiO_2 photocatalytic reduction of nitrate. Appl. Catal. B Environ. 220, 597–606.

Ukisu, Y., 2015. Complete catalytic debromination of polybrominated diphenyl ethers over a silica-supported palladium nanoparticle catalyst. Environ. Chem. Lett. 13, 211–216.

Ukisu, Y., Miyadera, T., 1997. Hydrogen-transfer hydrodehalogenation of aromatic halides with alcohols in the presence of noble metal catalysts. J. Mol. Catal. A Chem. 125, 135–142.

Wang, R., Li, H., Tao, X., Tang, T., Lin, H., Huang, K., et al., 2017a. Photodebromination behaviors of polybrominated diphenyl ethers in methanol/water systems: mechanisms and predicting descriptors. Sci. Total Environ. 595, 666–672.

Wang, R., Lu, G., Lin, H., Huang, K., Tang, T., Xue, X., et al., 2017b. Relative roles of H-atom transfer and electron transfer in the debromination of polybrominated diphenyl ethers by palladized nanoscale zerovalent iron. Environ. Pollut. 222, 331–337.

Wang, R., Tang, T., Lu, G., Huang, K., Yin, H., Lin, Z., et al., 2018a. Rapid debromination of polybrominated diphenyl ethers (PBDEs) by zero valent metal and bimetals: mechanisms and pathways assisted by density function theory calculation. Environ. Pollut. 240, 745–753.

Wang, Y., Zhu, Q., Wei, Y., Gong, Y., Chen, C., Song, W., et al., 2018b. Catalytic hydrogenation over supported gold: electron transfer versus hydride transfer. Appl. Catal. B Environ. 231, 262–268.

Wang, R., Tang, T., Lu, G., Zheng, Z., Huang, K., Li, H., et al., 2019a. Mechanisms and pathways of debromination of polybrominated diphenyl ethers (PBDEs) in various nano-zerovalent iron-based bimetallic systems. Sci. Total Environ. 661, 18–26.

Wang, R., Tang, T., Wei, Y., Dang, D., Huang, K., Chen, X., et al., 2019b. Photocatalytic debromination of polybrominated diphenyl ethers (PBDEs) on metal doped TiO_2 nanocomposites: mechanisms and pathways. Environ. Int. 127, 5–12.

Wang, X., Hu, Z., Chen, K., Dong, H., Li, S., Li, X., et al., 2019c. Efficient photocatalytic debromination of 2,2',4,4'-tetrabromodiphenyl ether by Ag-loaded CdS particles under visible light. Chemosphere 220, 723–730.

Wang, R., Zhu, Z., Tan, S., Guo, J., Xu, Z., 2020. Mechanochemical degradation of brominated flame retardants in waste printed circuit boards by ball milling. J. Hazard. Mater. 385, 121509.

Wang, X., Maeda, K., Thomas, A., Takanabe, K., Xin, G., Carlsson, J.M., et al., 2009. A metal-free polymeric photocatalyst for hydrogen production from water under visible light. Nat. Mater. 8, 76–80.

Watanabe, I., Tatsukawa, R., 1987. Formation of brominated dibenzofurans from the photolysis of flame retardant decabromobiphenyl ether in hexane solution by UV and sun light. Bull. Environ. Contam. Toxicol. 39, 953–959.

Wei, X., Guo, Z., Yin, H., Yuan, Y., Chen, R., Lu, G., et al., 2021. Removal of heavy metal ions and polybrominated biphenyl ethers by sulfurized nanoscale zerovalent iron: compound effects and removal mechanism. J. Hazard. Mater. 414, 125555.

Wei, Y., Gong, Y., Zhao, X., Wang, Y., Duan, R., Chen, C., et al., 2019. Ligand directed debromination of tetrabromodiphenyl ether mediated by nickel under visible irradiation. Environ. Sci. Nano 6, 1585–1593.

Wemken, N., Drage, D.S., Abdallah, M.A., Harrad, S., Coggins, M.A., 2019. Concentrations of brominated flame retardants in indoor air and dust from Ireland reveal elevated exposure to decabromodiphenyl ethane. Environ. Sci. Technol. 53, 9826–9836.

Xie, Q., Chen, J., Shao, J., Chen, C., Zhao, H., Hao, C., 2009. Important role of reaction field in photodegradation of deca-bromodiphenyl ether: theoretical and experimental investigations of solvent effects. Chemosphere 76, 1486–1490.

Xiong, P., Yan, X., Zhu, Q., Qu, G., Shi, J., Liao, C., et al., 2019. A review of environmental occurrence, fate, and toxicity of novel brominated flame retardants. Environ. Sci. Technol. 53, 13551–13569.

Xu, Y., Liang, C., Zhang, T., Tao, X., Wang, R., Huang, K., et al., 2020. Debromination of polybrominated diphenyl ethers (PBDEs) by palladized zerovalent zinc particles: influence factors, pathways and mechanism. Chemosphere 253, 126726.

Yao, B., Luo, Z., Zhi, D., Hou, D., Luo, L., Du, S., et al., 2021. Current progress in degradation and removal methods of polybrominated diphenyl ethers from water and soil: a review. J. Hazard. Mater. 403, 123674.

Yu, K., Sheng, G.D., McCall, W., 2016. Cosolvent effects on dechlorination of soil-sorbed polychlorinated biphenyls using bentonite clay-templated nanoscale zero valent iron. Environ. Sci. Technol. 50, 12949–12956.

Yu, L., Han, Z., Liu, C., 2015. A review on the effects of PBDEs on thyroid and reproduction systems in fish. Gen. Comp. Endocr. 219, 64–73.

Yu, L., Lam, J.W., Guo, Y., Wu, R.S., Lam, P.S., Zhou, B., 2011. Parental transfer of polybrominated diphenyl ethers (PBDEs) and thyroid endocrine disruption in zebrafish. Environ. Sci. Technol. 45, 10652–10659.

Zhang, L., Li, J., Zhao, Y., Li, X., Wen, S., Shen, H., et al., 2013. Polybrominated diphenyl ethers (PBDEs) and indicator polychlorinated biphenyls (PCBs) in foods from China: levels, dietary intake, and risk assessment. J. Agric. Food Chem. 61, 6544–6551.

Zhang, Y., Xi, B., Tan, W., 2021. Release, transformation, and risk factors of polybrominated diphenyl ethers from landfills to the surrounding environments: a review. Environ. Int. 157, 106780.

Zhang, Z., Wang, N., Zhu, L., Lv, H., Dong, X., Chai, H., et al., 2017. Synergistic effect between Fe and Bi_2O_3 on enhanced mechanochemical treatment of decabromodiphenyl ether. J. Environ. Chem. Eng. 5, 915–923.

Zhao, C., Yan, M., Zhong, H., Liu, Z., Shi, L., Chen, M., et al., 2018. Biodegradation of polybrominated diphenyl ethers and strategies for acceleration: a review. Int. Biodeterior. Biodegrad. 129, 23–32.

Zheng, Z., Lu, G., Wang, R., Huang, K., Tao, X., Yang, Y., et al., 2019. Effects of surfactant on the degradation of 2,2',4,4'-tetrabromodiphenyl ether (BDE-47) by nanoscale Ag/Fe particles: kinetics, mechanisms and intermediates. Enviorn. Pollut. 245, 780–788.

Zhou, C., Pagano, J., McGoldrick, D., Chen, D., Crimmins, B., Hopke, P., et al., 2019. Legacy polybrominated diphenyl ethers (PBDEs) trends in top predator fish of the Laurentian great lakes (GL) from 1979 to 2016: will concentrations continue to decrease? Environ. Sci. Technol. 53, 6650–6659.

Zhuang, Y., Ahn, S., Luthy, R.G., 2010. Debromination of polybrominated diphenyl ethers by nanoscale zerovalent iron: pathways, kinetics, and reactivity. Environ. Sci. Technol. 44, 8236–8242.

Zhuang, Y., Ahn, S., Seyfferth, A.L., Masue-Slowey, Y., Fendorf, S., Luthy, R.G., 2011. Dehalogenation of polybrominated diphenyl ethers and polychlorinated biphenyl by bimetallic, impregnated, and nanoscale zerovalent iron. Environ. Sci. Technol. 45, 4896–4903.